Vasohibin1, a new IRES trans-acting factor for sequential induction of angiogenic factors in hypoxia

Fransky Hantelys[1], Anne-Claire Godet[1], Florence Tatin[1], Edith Renaud-Gabardos[1], Françoise Pujol[1], Isabelle Ader[2], Laetitia Ligat[3], Anthony Henras[4], Eric Lacazette[1], Angelo Parini[1], Barbara Garmy-Susini[1], and Anne-Catherine Prats[1§]

[1]UMR 1048-I2MC, Inserm, Université de Toulouse, UPS, Toulouse, France.
[2]UMR 5273-STROMALAB, CNRS, Inserm, Université de Toulouse, UPS, Toulouse, France.
[3]UMR 1037-CRCT, Inserm, CNRS, Université de Toulouse, UPS, Pôle Technologique-Plateau Protéomique, Toulouse, France.
[4]UMR 5099-LBME, CBI, CNRS, Université de Toulouse, UPS, Toulouse, France.

[§]Corresponding author.
Contact information : Anne-Catherine Prats, Institut des Maladies Métaboliques et Cardiovasculaires, 1, Avenue Jean Poulhes, BP 84225, 31432 Toulouse cedex 4, France (e-mail: Anne-Catherine.Prats@inserm.fr)

Running title: IRESs, translational regulons in hypoxia

ABSTRACT
Hypoxia, a major inducer of angiogenesis, is known to trigger major changes of gene expression at the transcriptional level. Furthermore, global protein synthesis is blocked while internal ribosome entry sites (IRES) allow specific mRNAs to be translated. Here we report the transcriptome and translatome signatures of (lymph)angiogenic genes in hypoxic HL-1 cardiomyocytes: most genes are not induced at the transcriptome-, but at the translatome level, including all IRES-containing mRNAs. Our data reveal sequential activation of (lymph)angiogenic mRNA IRESs in early hypoxia. We identify vasohibin1 (VASH1) as an IRES trans-acting factor (ITAF) able to activate the earliest induced FGF1 IRES while it inhibits the other IRESs. Thus this new ITAF may have opposite effects on IRES activities in the steps of early hypoxia. These data suggest that IRESome composition varies at different stages of hypoxia, leading to sequential induction of (lymph)angiogenic factors required to form new functional vessels in ischemic heart.

Key words: cardiomyocyte/ hypoxia / IRES/ translational control/ vasohibin

INTRODUCTION
Hypoxia constitutes a major stress in different pathologies including cancer, as well as ischemic pathologies where artery occlusion leads to hypoxic conditions. In all these pathologies, hypoxia induces a cell response that stimulates angiogenesis to re-feed starved cells with oxygen and nutrients [1]. Recently it has been shown that lymphangiogenesis is also induced by hypoxia [2]. Hypoxia-induced (lymph)angiogenesis is mediated by strong modification of gene expression at both transcriptional and post-transcriptional levels [1,3]. A major way of gene expression regulation is mediated at the transcriptional level by the hypoxia induced factor 1 (HIF1), a transcription factor stabilized by oxygen deprivation, that activates transcription from promoters containing hypoxia responsive elements (HRE). One of the well-described HIF1 targets is vascular endothelial growth factor A (VEGFA), a major angiogenic factor [4,5]. However, two

other major angiogenic or lymphangiogenic growth factors, fibroblast growth factor 2 (FGF2) and VEGFC, respectively, are induced by hypoxia in a HIF-independent manner by a translational mechanism, indicating the importance of the post-transcriptional regulation of gene expression in this process [2,6].

Translational control of gene expression plays a crucial role in the stress response. In particular, translation of most mRNAs, occurring by the classical cap-dependent mechanism, is silenced whereas alternative translation mechanisms allow enhanced expression of a small group of messengers involved in the control of cell survival [3,7,8]. One of the major alternative mechanisms able to overcome this global inhibition of translation by stress depends on internal ribosome entry sites (IRESs) that correspond to RNA structural elements allowing the direct recruitment of the ribosome on mRNA. As regards the molecular mechanisms of IRES activation by stress, several studies have reported the involvement of RNA binding proteins, called IRES trans-acting factors (ITAFs), able to stabilize the adequate RNA conformation allowing ribosome recruitment [9-12]. Interestingly, subcellular relocalization of ITAFs plays a critical role in IRES-dependent translation [13]. Indeed, many RNA-binding proteins are known to shuttle between nucleus and cytoplasm, and it has been reported that cytoplasmic relocalization of ITAFs such as PTB, PCBP1, RBM4 or nucleolin is critical to activate IRES-dependent translation [12,13]. In contrast, other ITAFs such as hnRNPA1, may have a negative impact on IRES activity when accumulating in the cytoplasm [14]. However, how ITAFs participate in the regulation of the hypoxic response remains a challenging question to address.

IRESs are present in the mRNAs of several (lymph)angiogenic growth factors in the FGF and VEGF families, suggesting that the IRES-dependent mechanism might be a major way to activate angiogenesis and lymphangiogenesis during stress [2,12,15-18]. However, most studies of the role of hypoxia in gene expression regulation have been performed in tumoral hypoxia, while it has been reported that tumoral angiogenesis leads to formation of abnormal vessels that are non functional, which strongly differs from non tumoral angiogenesis that induces formation of functional vessels [19]. This suggests that gene expression regulation in response to hypoxia may be different in cancer versus ischemic pathologies. In particular, the role of IRESs in the control of gene expression in ischemic heart, the most frequent ischemic pathology, remains to be elucidated.

Here we analyzed the transcriptome and the translatome of (lymph)angiogenic growth factors in hypoxic cardiomyocytes, and studied regulation of IRES activities in early and late hypoxia. Data show that in cardiomyocyte, (lymph)angiogenic growth factors are mostly regulated at the translational level. Interestingly, FGF and VEGF mRNA IRESs are sequentially activated at different times of early hypoxia in contrast to IRESs of non angiogenic messengers. We also looked for ITAFs governing IRES activation in hypoxia and identified vasohibin1 (VASH1) as a new ITAF specific of the earliest activated FGF1 IRES in cardiomyocytes. VASH1 knock-down strongly down-regulates the earliest-induced FGF1 IRES but not the other IRESs, revealing that this protein is a new IRES trans-acting factor (ITAF) in cardiomyocytes, specific of early hypoxia.

RESULTS

Most (lymph)angiogenic genes are not induced at the transcriptome level of hypoxic cardiomyocytes.

In order to analyze expression of angiogenic and lymphangiogenic growth factors in hypoxic cardiomyocytes, the HL-1 cell line was chosen: although immortalized, it keeps the beating phenotype specific to cardiomyocyte [20]. HL-1 cells were submitted to increasing times of hypoxia, from 5 minutes to 24 hours and their trancriptome was analyzed on a Fluidigm Deltagene PCR array targeting 96 genes of angiogenesis, lymphangiogenesis and/or stress (Fig. 1, EV Fig. 1, EV Table 1). Data showed a significant increase of *Vegfa*, PAI-1 and apelin (*Apln*) mRNA levels, with a peak at 8h of hypoxia for *Vegfa* and PAI1 and 24h for *Apln*. These three

genes are well described HIF1 targets [4,21,22]. However, only 5-8% of the genes were induced, while the mRNA levels of several major angio- or lymphangiogenic factors, such as FGF2 and VEGFC, were strongly decreased after 4h or 8h of hypoxia. These data indicate that the transcriptional response to hypoxia in cardiomyocytes is not the major mechanism controlling expression of (lymph)angiogenic factors, suggesting that post-transcriptional mechanisms are involved.

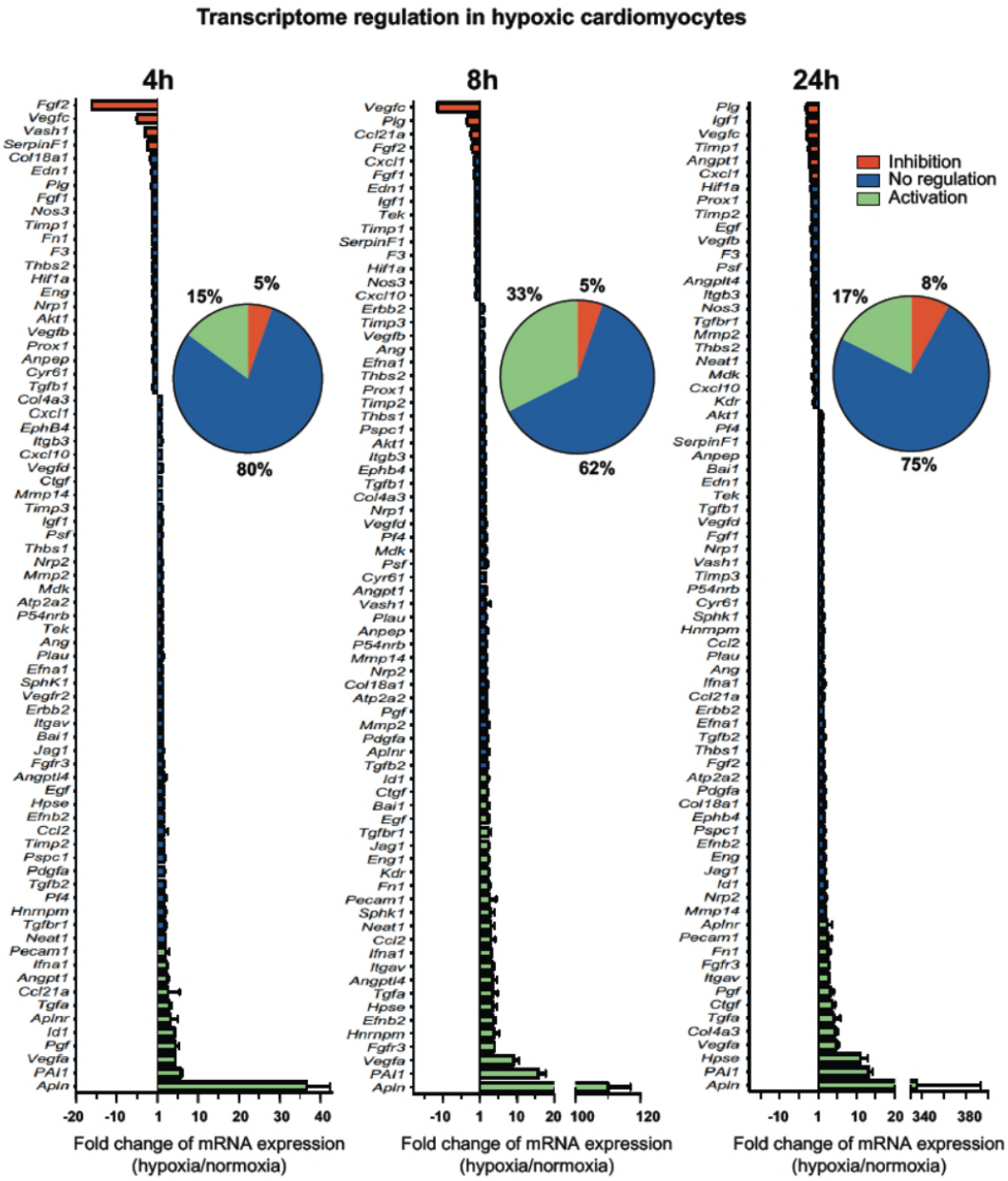

Figure 1. Most (lymph)angiogenic genes are not induced at the transcriptome level in hypoxic cardiomyocytes.

Total RNA was purified from HL-1 cardiomyocytes submitted to increasing times from 5 min to 24 h of hypoxia at 1% O_2, as well as from normoxic cardiomyocytes as a control. cDNAs were synthesized and used for a Fluidigm deltagene PCR array dedicated to genes related to (lymph)angiogenesis or stress (EV Table 4). Relative quantification (RQ) of gene expression during hypoxia was calculated using the $2^{-\Delta\Delta CT}$ method with normalization to 18S and to normoxia. mRNA levels are presented by histograms for the times of 4 h, 8 h and 24 h, as the fold change of repression (red) or induction (green) normalized to normoxia. Non-regulated mRNAs are represented in blue. When the RQ value is inferior to 1, the fold change is expressed as -1/RQ. The percentage of repressed, induced, and non-regulated mRNAs is indicated for each time. For earlier times of 5 min to 2 hr, the percentages are shown in EV Fig. 1. The detailed values for all the times of the kinetics are presented in EV Table 1.

mRNAs of most (lymph)angiogenic genes are recruited into polysomes in hypoxic cardiomyocytes.

Based on the fact that mRNA present in polysomes are actively translated, we tested the hypothesis of translational induction by analysing the recruitment of mRNAs into polysomes. This experiment was performed in early hypoxia (4 hr). The polysome profile displayed, as expected, a strong decrease of global translation (Fig. 2A). In contrast, 94% of the genes of the (lymph)angiogenic array showed a more sustained recruitment into polysomes under hypoxic conditions (Fig. 2B, EV Table 2). This translational induction not only targets major angiogenic factors and their receptors (*Vegfa, Fgf1, Pdgfa, Fgfr3, Kdr*...), but also genes involved in cardiomyocyte survival in ischemic heart (*Igf1, Igf1R*) or in inflammation (BAI1, *Tgfb*). These data suggest that in cardiomyocytes, the main response to early hypoxia of (lymph)angiogenic genes is not transcriptional, but translational.

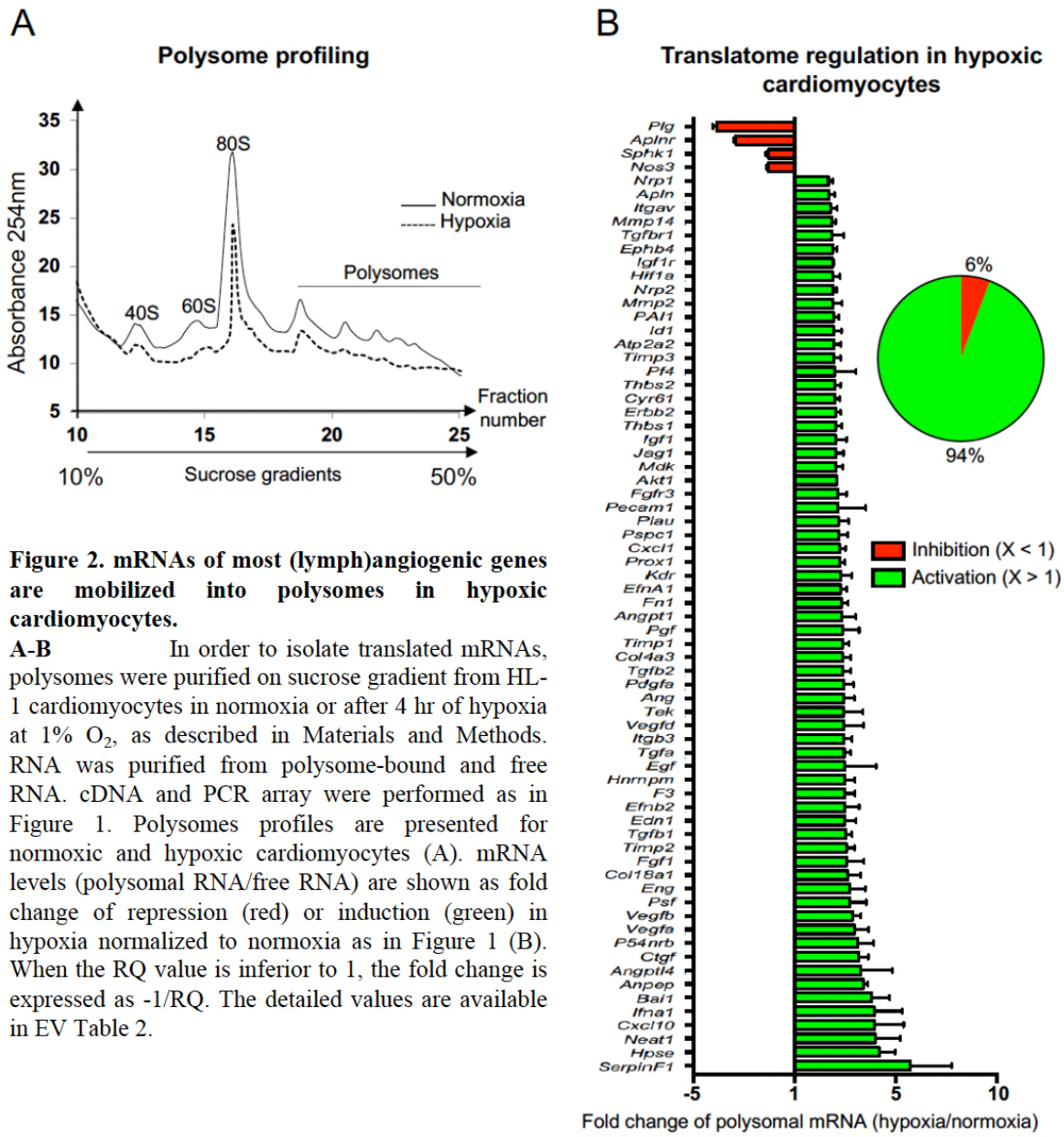

Figure 2. mRNAs of most (lymph)angiogenic genes are mobilized into polysomes in hypoxic cardiomyocytes.

A-B In order to isolate translated mRNAs, polysomes were purified on sucrose gradient from HL-1 cardiomyocytes in normoxia or after 4 hr of hypoxia at 1% O_2, as described in Materials and Methods. RNA was purified from polysome-bound and free RNA. cDNA and PCR array were performed as in Figure 1. Polysomes profiles are presented for normoxic and hypoxic cardiomyocytes (A). mRNA levels (polysomal RNA/free RNA) are shown as fold change of repression (red) or induction (green) in hypoxia normalized to normoxia as in Figure 1 (B). When the RQ value is inferior to 1, the fold change is expressed as -1/RQ. The detailed values are available in EV Table 2.

IRES-containing mRNAs are more efficiently mobilized into polysomes under hypoxic conditions.

IRES-dependent translation has been reported to drive translation of several mRNAs in stress conditions [2,3,6,23]. Thus we focused onto the regulation of the different IRES-containing mRNAs present in the Fluidigm array (Fig. 3). Interestingly, the only IRES-containing mRNA to be significantly induced at the transcriptome level by hypoxia was *Vegfa* (Fig. 3A and EV Fig. 2). Expression of the apelin receptor (*Aplnr*), presumably devoid of IRES, is also shown for comparison.

Polysome recruitment of these IRES-containing mRNAs is shown in figure 3B. Clearly, *Fgf1, Vegfa, Vegfd, Hif1a, Igf1r* and *Cyr61* mRNAs were recruited into polysomes under hypoxia 2 to 4 times more than in normoxia, suggesting an important induction in terms of translation. In contrast, *Aplnr* mRNA recruited into polysomes decreased about three times. The data are not available for *Fgf2* and *Vegfc* mRNAs, which were not detectable. These results indicate that hypoxia in cardiomyocytes, although blocking global cap-dependent translation, induces translation of all detectable IRES-containing angiogenic factor mRNAs. This mechanism occurs as soon as 4 hours after oxygen deprivation, thus corresponding to an early event in the hypoxic response.

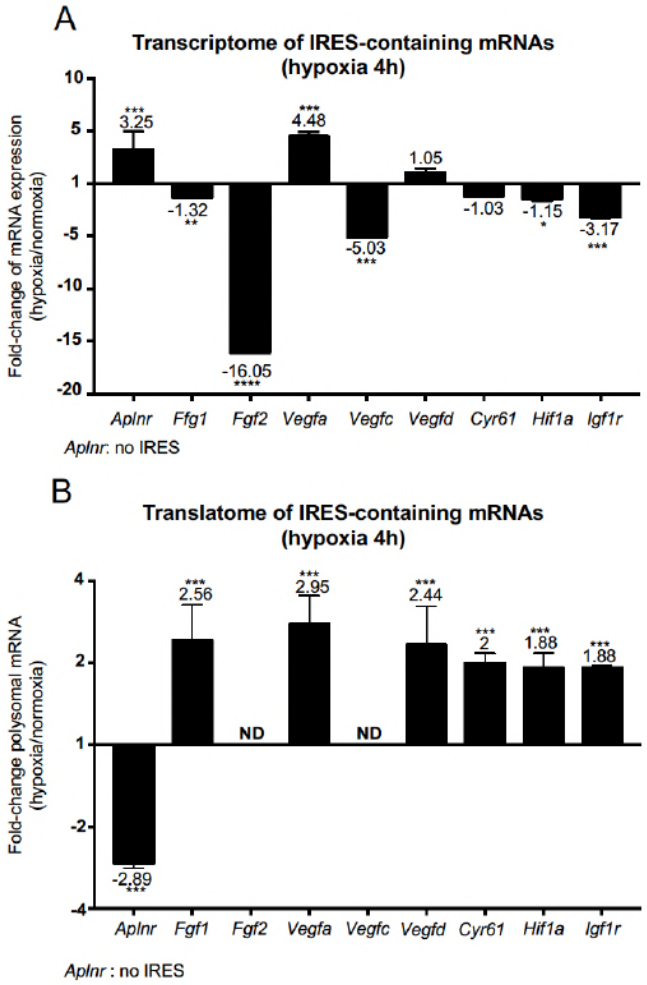

Figure 3. IRES-containing mRNAs are more efficiently associated to polysomes in hypoxic conditions.

A-B RQ values for IRES-containing mRNA transcriptome (A) and translatome (B) extracted from the PCR arrays shown in Figures 1 and 2. The gene *Aplnr* (apelin receptor) was chosen as a control without an IRES. *Vegfc* and *Fgf2* mRNAs, repressed in the transcriptome, were below the detection threshold in polysomes (ND). Histograms correspond to means of triplicate experiments ± standard error of the mean, *p<0.05, **p<0.01, ***<0.001, ****p<0.0001 compared to normoxia.

IRESs are sequentially activated during hypoxia.

To confirm that the polysome recruitment of IRES-containing mRNAs actually corresponds to a stimulation of IRES-dependent translation, IRESs from FGF and VEGF mRNAs were introduced into a bicistronic dual luciferase gene expression cassette (Fig. 4A). As controls, two IRESs from non angiogenic mRNAs, c-myc and EMCV IRESs, were used. The well established bicistronic vector strategy, previously validated by us and others, allows to measure

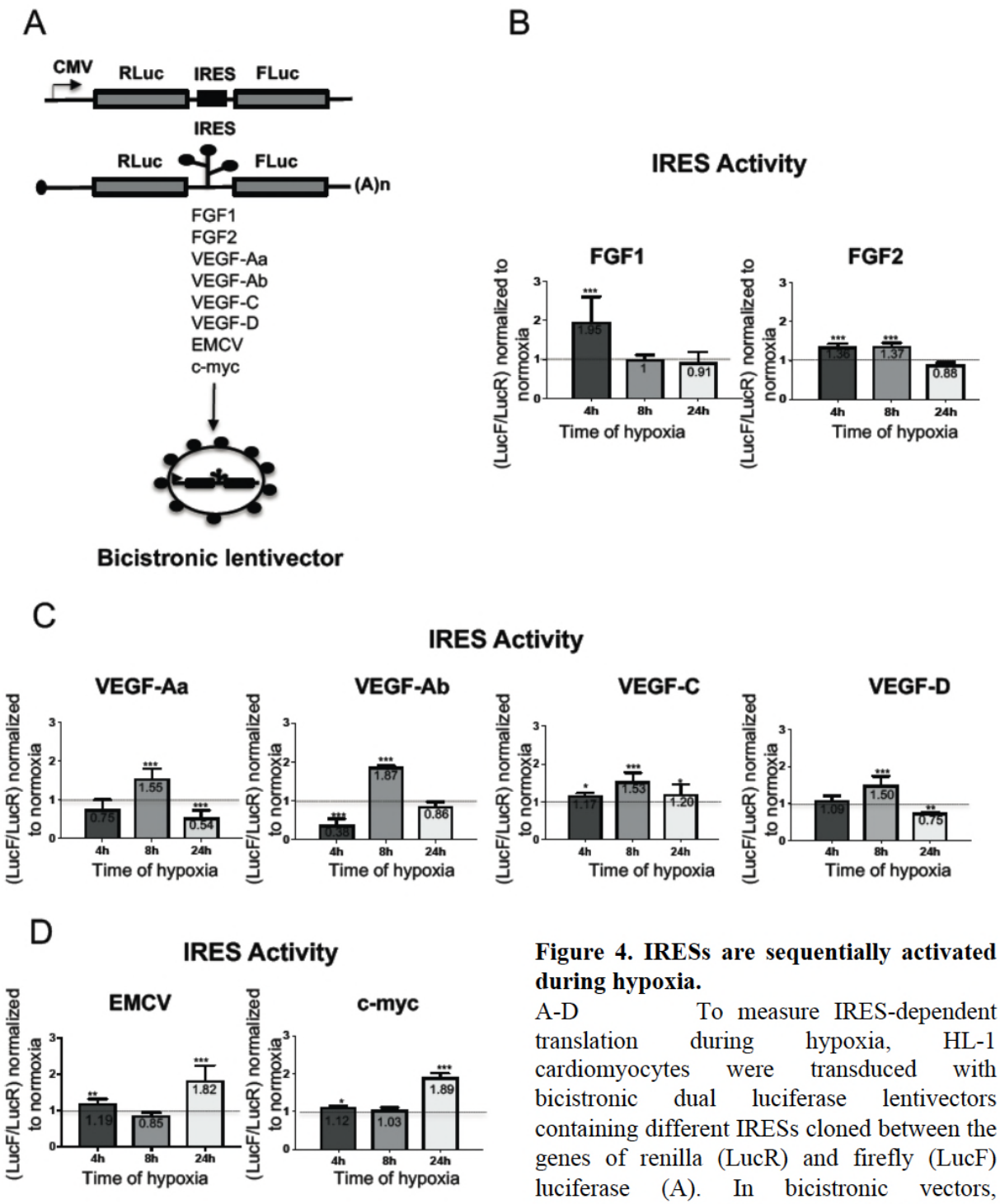

Figure 4. IRESs are sequentially activated during hypoxia.

A-D To measure IRES-dependent translation during hypoxia, HL-1 cardiomyocytes were transduced with bicistronic dual luciferase lentivectors containing different IRESs cloned between the genes of renilla (LucR) and firefly (LucF) luciferase (A). In bicistronic vectors, translation of the first cistron LucR is cap-dependent whereas translation of the second cistron LucF is IRES-dependent [24]. Transduced cardiomyocytes were submitted to 4h, 8h or 24h of hypoxia and luciferase activities measured. IRES activities during hypoxia, expressed as LucF/LucR ratio, are normalized to normoxia. Three groups of activation were identified: FGF IRESs (B), VEGF IRESs (C), non-angiogenic IRESs (D) at 4h, 8h or 24h of hypoxia, respectively.

Histograms correspond to means ± standard error of the mean, *p<0.05, **p<0.01, ***<0.001, compared to normoxia. Experiments have been reproduced from 3 to 10 times (depending on the IRES) and for each IRES a representative triplicate experiment is shown.

IRES activity revealed by expression of the second cistron, LucF [2,24]. The bicistronic cassettes were subcloned into lentivectors, as HL-1 cells are not efficiently transfected by plasmids but can be easily transduced by lentivectors with an efficiency of more than 80% (not shown). HL-1 cardiomyocytes were transduced by the different lentivectors and submitted to increasing times of hypoxia. Luciferase activities were measured from cell extracts and IRES activities reported as the LucF/LucR luminescence ratio. Results showed different IRES behaviors (Fig. 4B-D). Clearly, the FGF1 and FGF2 IRESs were induced early, after 4 hours of oxygen deprivation (Fig. 4B). The FGF1 IRES showed a peak at 4 hours, while the FGF2 IRES, even more moderately activated, displayed a sustained activity after 8 hours. In contrast, the four VEGF IRESs all peaked after 8 hours of hypoxia (Fig. 4C). Finally, the c-myc and EMCV IRESs were activated only in late hypoxia after 24 hours (Fig. 4D). These data provide two important information: first, IRESs from (lymph)angiogenic growth factor mRNAs are activated during early hypoxia, in contrast to other IRESs. Second, these "angiogenic" IRESs are sequentially activated during early hypoxia. The earliest wave concerns the FGF IRESs, especially FGF1 IRES, followed by a second wave of activation of the VEGF IRESs.

Identification of IRES-bound proteins in hypoxic cardiomyocytes reveals vasohibin1 as a new RNA-binding protein.

The sequential activation of the angiogenic factor IRESs in early hypoxia suggested that different ITAFs may be involved at 4 hours and at 8 hours. In an attempt to identify such ITAFs, we used the technology of biomolecular analysis coupled to mass spectrometry (BIA-MS), validated for ITAF identification in two previous studies [12,25]. Biotinylated RNAs corresponding to FGF1 (4 hr activation), VEGFAa (8 hr activation) and EMCV IRESs (24h activation) were used as probes for BIA-MS. Hooked proteins from normoxic and hypoxic HL-1 cells were then recovered and identified (Fig. 5A-B, EV Table 3). Surprisingly, except for nucleolin bound to the VEGFA IRES in normoxia, no known ITAF was identified as bound to these IRESs in normoxia or in hypoxia. Interestingly, besides several proteins unrelated to (lymph)angiogenesis, we detected the presence of vasohibin1 (VASH1), a protein described as an endothelial cell-produced angiogenesis inhibitor, but also for its role in stress tolerance and cell survival [26,27](Fig. 5C). However, this secreted protein has never been reported for any RNA-binding activity. VASH1 bound to the FGF1 IRES under hypoxia, but not under normoxia (EV Table 3). This protein also bound to the EMCV IRES both in normoxia and hypoxia but not to the VEGFA IRES, showing a selective binding depending on the IRES and the stress condition. In order to address the RNA binding potential of VASH1, we performed an *in silico* analysis of VASH1 protein sequence that predicted two conserved RNA-binding domains (RBD) in the N- and C-terminal parts of the full length protein, respectively (Fig. 5D, EV Fig. 3A and 3B). The direct interaction of VASH1 with the FGF1 IRES was assessed by surface plasmon resonance using a recombinant protein containing the N-terminal predicted RBD1, resulting in the measurement of an affinity constant of 2.79 μM (Fig. 5E and 5F). These data strongly suggest that the VASH1 predicted RBD1 exhibits an RNA binding activity, while it can be expected that the affinity would be reinforced in the presence of the C-terminal RBD.

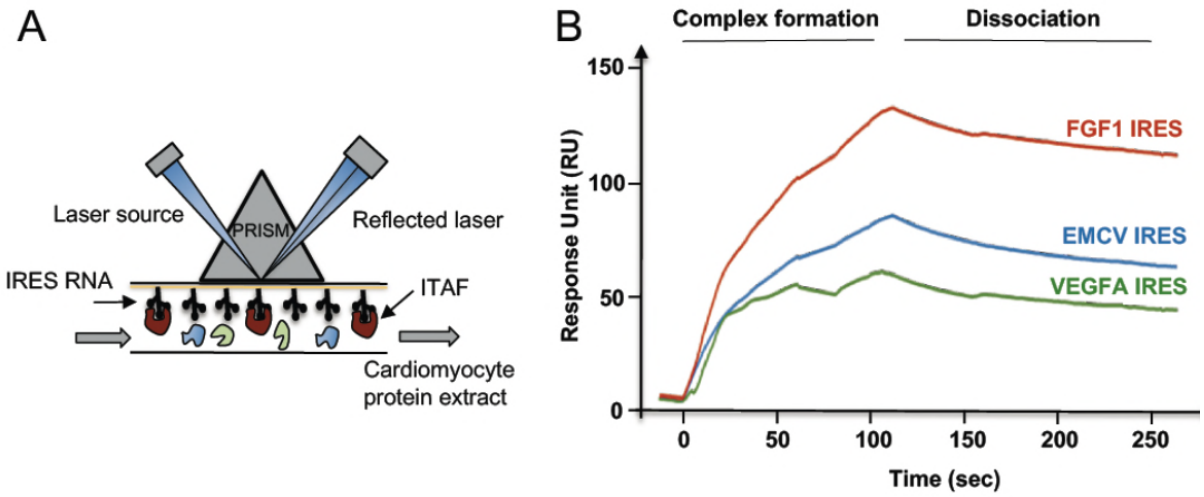

C **Proteins bound to FGF1 IRES RNA**

ID	4h hypoxia Description
ASAP2	Arf-GAP with SH3 domain, ANK repeat and PH domain-containing protein 2
ATPA	ATP synthase subunit alpha, mitochondrial
C2C2L	C2 domain-containing protein 2-like
PDE8B	High affinity cAMP-specific and IBMX-insensitive 3~,5~-cyclic phosphodiesterase 8B
GVIN1	Interferon-induced very large GTPase 1
ACOX1	Peroxisomal acyl-coenzyme A oxidase 1
TAM41	Phosphatidate cytidylyltransferase, mitochondrial
ALBU	Serum albumin
TCPG	T-complex protein 1 subunit gamma
VASH1	Vasohibin-1

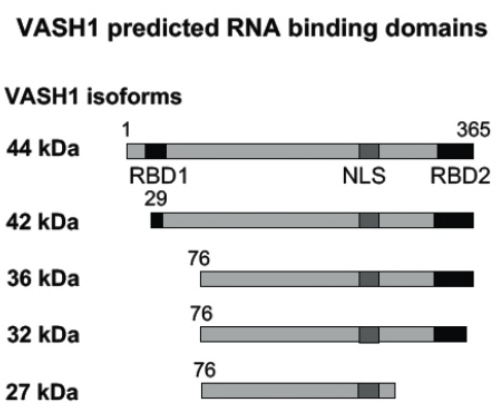

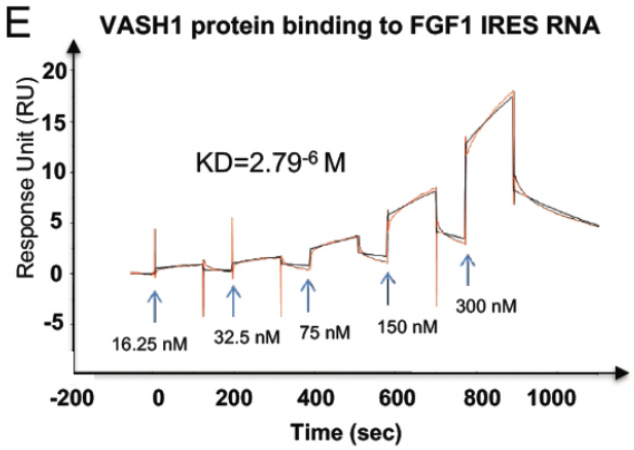

Figure 5. Identification of IRES-bound proteins in hypoxic cardiomyocytes reveals vasohibin1 as a new RNA-binding protein.

A-C Biotinylated IRES RNAs were transcribed *in vitro* and immobilized on the sensorchip of the BIAcore T200 optical biosensor device (A). Total cell extracts from normoxic or hypoxic HL-1 cardiomyocytes were injected (B). Bound proteins were recovered as described in Mat. & Meth. and identified by mass spectrometry (LC-MS/MS) after tryptic digestion. Proteins bound to the FGF1 IRES after 4h of hypoxia are shown (C). The complete list of proteins bound in normoxia and and hypoxia to FGF1, VEGFAa and EMCV IRESs is shown in EV Table 3.

D-E VASH RNA-binding properties. Diagrams of the VASH1 isoforms described by Sonoda et al **[34]**. The predicted RNA binding domains and NLS identified *in silico* in EV Figure 3, conserved in mouse and human, are indicated (D). Recombinant VASH1 was injected into the Biacore T200 device containing immobilized FGF1 IRES as above (E). The affinity constant (KD) was calculated (F) with a Single Cycle Kinetics (SCK) strategy.

Vasohibin1 is translationally induced and nuclearized in early hypoxia.

VASH1 has been previously described for its expression in endothelial cells but never in cardiomyocytes [26]. The present BIA-MS study provides evidence that it is expressed in HL-1 cardiomyocytes (EV Table 3). We analyzed the regulation of VASH1 expression during hypoxia: *Vash1* mRNA level strongly decreases after 4 hours of hypoxia whereas it is slightly upregulated after 8 hours (Fig. 1, EV Table 1, Fig. 6A). In contrast, analysis of *Vash1* mRNA recruitment into polysomes showed a strong increase at 4h of hypoxia (about 7 times), indicating that *Vash1* mRNA translation is strongly induced (Fig. 2B, EV Table 2, Fig. 6B).

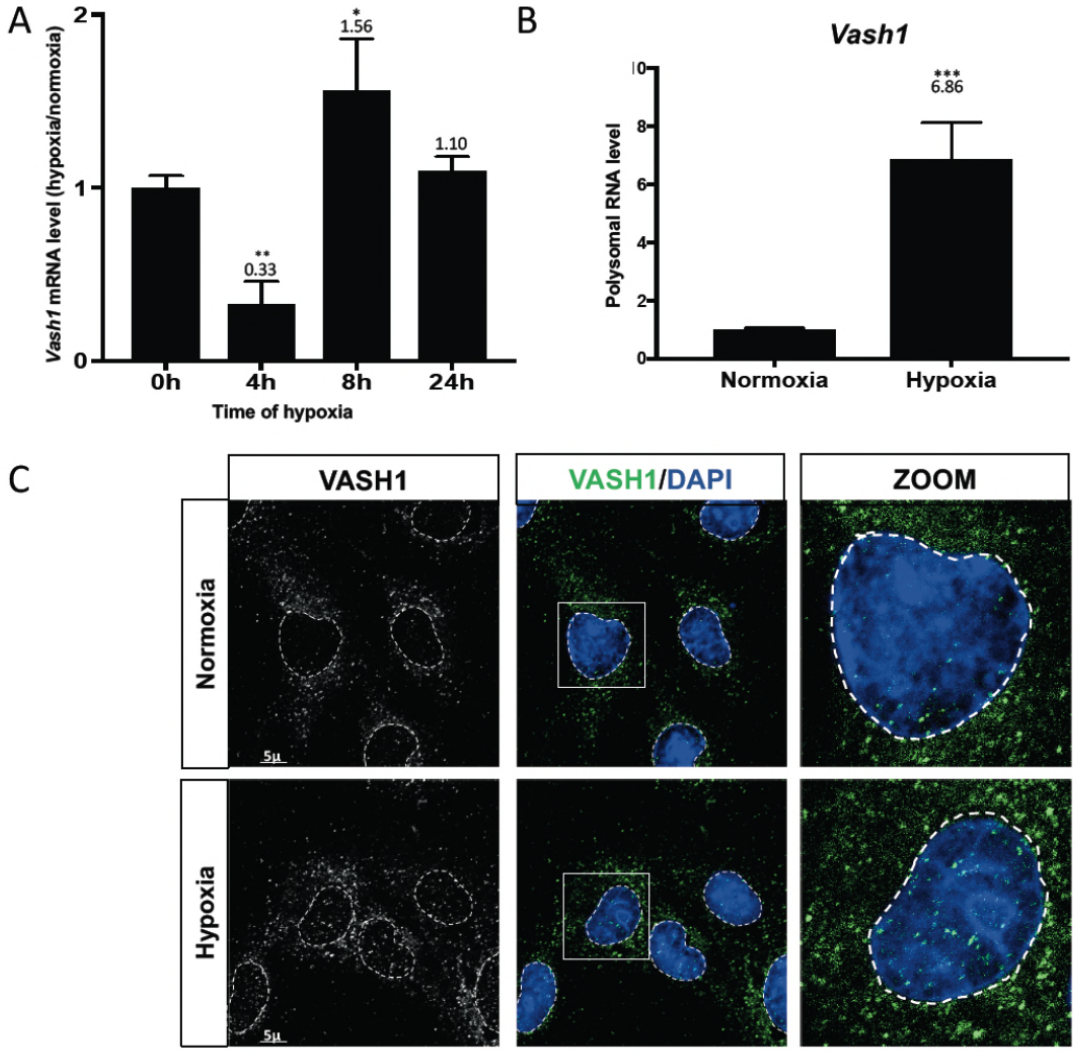

Figure 6. Vasohibin1 is translationally induced and nuclearized in early hypoxia.

A-B VASH1 expression was analyzed by RT-qPCR in HL-1 cardiomyocytes in response to hypoxia at the transcriptome and translatome levels. Total RNA was purified from cardiomyocytes in normoxia, or submitted to 4 h, 8 h or 24 h of hypoxia (A). Polysomal RNA was purified from cardiomyocytes in normoxia or after 4 h of hypoxia (B).

Histograms correspond to means ± standard error of the mean, *p<0.05, **p<0.01, ***<0.001, compared to normoxia. Experiments have been reproduced 3 times independently and a representative triplicate experiment is shown.

C VASH1 was immunodetected in HL-1 cardiomyocytes in normoxia or after 4h of hypoxia. DAPI staining allows to detect VASH1 nuclear localization (MERGE).

VASH1 immunodetection confirmed a strong expression of VASH1 at 4h of hypoxia, despite the decrease of its mRNA. In normoxia, VASH1 appeared as a mainly cytoplasmic protein,

with a perinuclear localization that could correspond to the endoplasmic reticulum (Fig. 6C). In contrast, after 4h of hypoxia numerous foci of VASH1 appeared in the nucleus.
Even though this result was unexpected, as VASH1 is described as a secreted protein, VASH1 nuclearization was however supported by the in silico identification of a fully conserved nuclear localization sequence (NLS) HVLKKVKLG (Fig. 5D, EV Fig. 3C and 3D).

Vasohibin1 is a new ITAF selectively active in early hypoxia.
The putative ITAF function of VASH1 was assessed by a knock-down approach using an siRNA smartpool (siVASH1). Transfection of HL-1 cardiomyocytes with siVASH1 was able to knock down VASH1 mRNA with an efficiency of 73% (Fig. 7A and 7B). The effect of VASH1 knock-down was analyzed in HL-1 cells transduced with different IRES-containing bicistronic lentivectors and submitted to 4h of hypoxia. The results showed that the FGF1 IRES activity decreases by 80% upon VASH1 knock-down under hypoxia, whereas the other IRESs where less drastically affected (Fig. 7C). The EMCV IRES is slightly inhibited by the knock-down, in concordance with the ability of VASH1 to bind this IRES (EV Table 3). Interestingly, the FGF2, VEGFA, -C and D IRESs where stimulated, suggesting that VASH may also have an inhibitory effect. These data suggest that VASH1 is an ITAF active in early hypoxia (4 hours), required for activation of the FGF1 IRES, while showing an inhibitory effect on other tested growth factor IRES activities (Fig. 7D).
In order to evaluate the possibility of a wider role of VASH1 on translational control, the (lymph)angiogenic factor mRNA polysome profile was analyzed in siVASH1-treated HL-1 cells as in Figure 2 (EV Table 2, right column). VASH1 knock-down decreased mobilization into polysomes of several IRES mRNAs including the *Ffg1* and *Igf1r* mRNA, while it increased the recruitment other IRES-containing mRNAs, including *Hif1a*, *Vegfa* and *Vegfd*, in concordance with the data of Fig. 7. A few mRNAs without a known IRES such as *Apln*, *Cxcl10* or *Hpse* had also a strongly decreased polysome profile upon VASH1 depletion, suggesting a wide impact of VASH1, direct or indirect, on (lymph)-angiogenic growth factor translation control.

DISCUSSION

The present study highlights the crucial role of translational control in cardiomyocyte response to hypoxia. Up to now, although a few genes had been described for their translational regulation by hypoxia, it was thought that most genes are transcriptionally regulated. Here we show that translational control, revealed by mRNA recruitment in polysomes during hypoxia, concerns the majority of the genes involved in angiogenesis and lymphangiogenesis. IRES-dependent translation appears as a key mechanism in this process, as we show that all the (lymph)angiogenic mRNAs known to contain an IRES are up-regulated. Furthermore, our data reveal that IRESs of angiogenic factor mRNAs are sequentially activated during early hypoxia. These waves of IRES activation indicate the involvement of different ITAFs, specific of these steps of early hypoxia. We have identified an angiogenesis-related protein, vasohibin1, as a new ITAF responsible for activation of the FGF1 IRES in the earliest wave of IRES activation.

Translational control in tumoral versus non tumoral hypoxia.
Most studies of gene expression in response to stress have been performed at the transcriptome level in tumoral cells of different origins, whereas the present study is focused on cardiomyocytes. HL-1 cardiomyocytes are immortalized but still exhibit the beating phenotype [20]. Thus this cell model, although not perfectly mimicking the cardiomyocyte behavior *in vivo*, is still close to a physiological state. The strong translational response to hypoxia revealed by our data, that differs from the transcriptional response usually observed in tumor cells, may reflect mechanisms occurring in cells that are not engaged into the cell transformation process

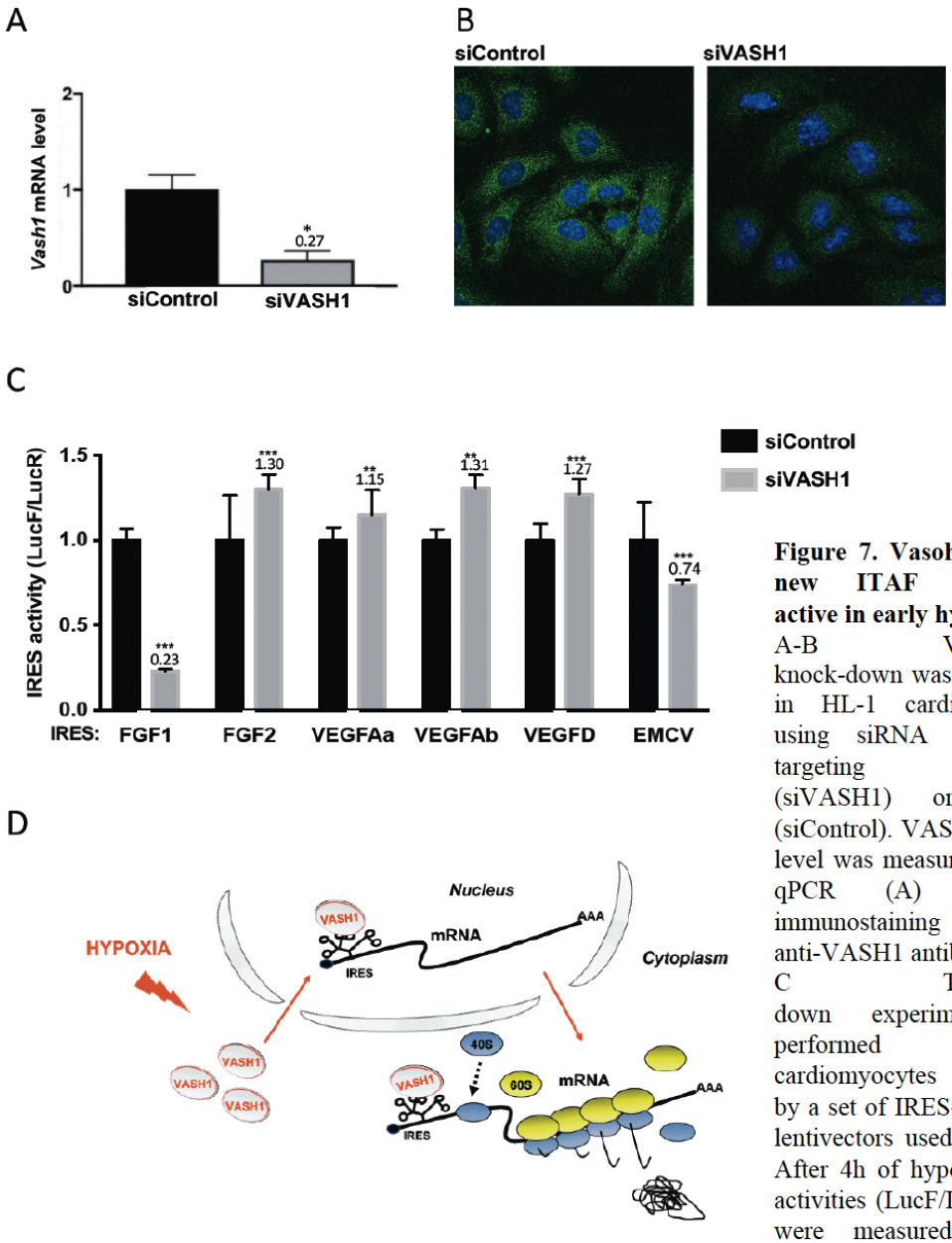

Figure 7. Vasohibin1 is a new ITAF selectively active in early hypoxia.
A-B VASH1 knock-down was performed in HL-1 cardiomyocytes using siRNA smartpools targeting VASH1 (siVASH1) or control (siControl). VASH1 mRNA level was measured by RT-qPCR (A) of by immunostaining using an anti-VASH1 antibody (B).
C The knock-down experiment was performed on cardiomyocytes transduced by a set of IRES-containing lentivectors used in Fig. 4. After 4h of hypoxia, IRES activities (LucF/LucR ratio) were measured in cell extracts. The IRES activity values have been normalized to the control siRNA. Histograms correspond to means ± standard error of the mean, *p<0.05, **p<0.01, ***<0.001, compared to siControl. The experiment was repeated 3 times independently and a representative triplicate experiment is shown.
D Model of mechanism for IRES activation by VASH1. Cytoplasmic VASH1 (maybe a specific isoform) is partly mobilized into nucleus where it binds to the mRNA IRES. IRESome is then exported into cytoplasm and VASH1 allows mRNA recruitment into polysomes, resulting in translation.

leading to cancer, or at least not too far. Indeed, HL-1 cells respond to hypoxia very early, whereas various murine or human tumor cell lines described in other reports require a longer time of hypoxia for IRES-dependent translation to be stimulated. In human breast cancer BT474 cells, VEGFA, HIF and EMCV IRESs are all activated after 24h of hypoxia [28]. In murine 4T1 and LLC cells (breast and lung tumor, respectively) as well as in human CAPAN-1 pancreatic adenocarcinoma, the VEGFA and VEGFC IRESs are activated after 24 hours of hypoxia whereas the EMCV IRES is not activated [2]. The same observation of late activation in 4T1 cells has been made for the FGF1 IRES, while this IRES is activated after 4 hours in HL-1 cardiomyocytes (Godet AC & Prats AC, unpublished data)(Fig. 4). Also, the VEGFD IRES is differently regulated in HL-1 cardiomyocytes compared to 4T1 tumor cells: only heat shock, but not hypoxia, is able to activate this IRES in 4T1 cells, whereas it is activated after 8

hours of hypoxia in HL-1 cardiomyocytes [12](Fig. 4). These observations suggest that many tumoral cell lines developing resistance to hypoxia are not able to govern subtle regulations of gene expression such as the waves of IRES regulation observed in HL-1 cells.

VASH1, an early hypoxic ITAF.

We also consider the hypothesis that the important process of translational regulation observed in our study may be cardiomyocyte-specific. In such a case, IRES-dependent translation would depend on cell type specific ITAFs as well as the early response to hypoxia. In agreement with this hypothesis, VASH1 expression is cell-type specific: described up to now as endothelial-specific, this protein is not expressed in tumoral cells [26]. In the present study, we show that this cell-type specificity extends to cardiomyocytes. Consistent with our data, this protein has been described as a key actor of striated muscle angio-adaptation [29]. VASH1 may thus have a role in the early hypoxic response in a limited number of cell types. The ITAF role of VASH1 identified here is physiologically relevant if one considers the VASH1 function in angiogenesis and stress tolerance [27]. Furthermore, it has been reported that VASH1 is induced after 3 hours of cell stress at the protein level but not at the transcriptional level in endothelial cells [30]. This is in agreement with our observation in cardiomyocytes where VASH1, although downregulated in the transcriptome at 4 hours of hypoxia, is more efficiently recruited in polysomes at the same time (Fig. 6).

It is noteworthy that VASH1 itself seems to be induced translationally by stress [30](Fig. 6). In endothelial cells, Myashita et al report that the protein HuR upregulates VASH1 by binding to its mRNA. HuR may bind to an AU-rich element present in the 3' untranslated region of the VASH1 mRNA. However, in other studies, HuR has also been described as an ITAF, thus it is possible that VASH1 itself may be induced by an IRES-dependent mechanism [31,32].

The anti-angiogenic function of VASH1 may appear inconsistent with its ability to activate the IRES of an angiogenic factor. However, our data also show that VASH1 might be an activator or an inhibitor for (lymph)angiogenic factor mRNA translation. Such a double role may explain the unique dual ability of VASH1 to inhibit angiogenesis and to promote endothelial cell survival [27,30]. This could result from the existence of different VASH1 isoforms of 44 kDa, 42 kDa, 36 kDa, 32 kDa and 27 kDa, resulting from alternative splicing and/protein processing [29,33-35]. Interestingly p42 and p27 are the main isoforms expressed in heart, while the p44 is undetectable [29,34]. One can expect that the ITAF function is carried by p42 which contains the two predicted RNA binding domains as well as the conserved NLS (Fig.5D, EV Fig. 3). Nuclear VASH1 observed during hypoxia suggests that it could bind to the IRES in the nucleus, as described for other ITAFs [25,36,37]. Several reports show that ITAF shuttling between cytoplasm and nucleus is critical for their activity. Previous reports mainly describe ITAFs as nuclear proteins that are relocalized into cytoplasm to drive IRES-dependent translation, as shown for RBM4, PTB, PCBP1 and nucleolin [2,13]. However cytoplasmic accumulation can also drive translation repression. This was demonstrated in the case of hnRNP A1 regulating the X-linked inhibitor of apoptosis IRES [14]. In normoxia, VASH1 is mostly cytoplasmic and secreted. We hypothesize that its ITAF activity may result from its nuclear relocalization under hypoxia to form the IRESome which is then exported from nucleus to cytoplasm to drive IRES-dependent translation (Fig. 7D).

IRESs as cis-acting regulons in the hypoxic response.

The different waves of IRES activation observed in the present study suggest that different subsets of IRESs function as cis-acting regulons during hypoxia. The concept of translational regulon has been revealed for the *Hox* gene family, whose mRNAs all contain IRESs that are regulated by ribosomal protein RPL38 [38].

Our data indicate that VASH1 participates in an IRESome able to activate the FGF1 IRES. We hypothesize that FGF1 might belong to a regulon of very early IRESs whereas the VEGF IRESs would constitute a regulon of mid-early IRESs. It is important to notice that the FGF2 IRES

behaves differently from the FGF1 IRES, as it remains activated at 8 hours. The composition of these different IRESome complexes is still to be discovered.

MATERIALS & METHODS

Lentivector construction and production

Bicistronic lentivectors coding for the *renilla* luciferase (LucR) and the stabilized firefly luciferase Luc+ (called LucF in the text) were constructed from the dual luciferase lentivectors described previously, which contained Luc2CP [2,12]. The cDNA sequences of the human FGF1, -2, VEGFA, -C, -D, c-myc and EMCV IRESs were introduced between the first (LucR) and the second cistron (LucF) [18,39,40]. The two IRESs of the VEGFA have been used and are called VEGFAa and VEGFAb, respectively [15]. The expression cassettes were inserted into the SIN lentivector pTRIP-DU3-CMV-MCS vector described previously [40]. All cassettes are under the control of the cytomegalovirus (CMV) promoter.

Lentivector particles were produced using the $CaCl_2$ method-based by tri-transfection with the plasmids pLvPack and pLvVSVg, $CaCl_2$ and Hepes Buffered Saline (Sigma-Aldrich, Saint-Quentin-Fallavier, France), into HEK-293FT cells. Viral supernatants were harvested 48 hours after transfection, passed through 0.45-µm PVDF filters (Dominique Dutscher SAS, Brumath, France) and stored in aliquots at -80°C until use. Viral production titers were assessed on HT1080 cells with serial dilutions and scored for GFP expression by flow cytometry analysis on a BD FACSVerse (BD Biosciences, Le Pont de Claix, France).

Cell culture, transfection and transduction

HEK-293FT cells and HT1080 cells were cultured in DMEM-GlutaMAX + Pyruvate (Life Technologies SAS, Saint-Aubin, France), supplemented with 10% fetal bovine serum (FBS), and MEM essential and non-essential amino acids (Sigma-Aldrich).

Mouse atrial HL-1 cardiomyocytes were a kind gift from Dr. William Claycomb (Department of Biochemistry & Molecular Biology, School of Medicine, New Orleans)[20]. HL-1 cells were cultured in Claycomb medium containing 10% FBS, Penicillin/Streptomycin (100U/mL-100µg/mL), 0.1mM norepinephrine, and 2mM L-Glutamine. Cell culture flasks were pre-coated with a solution of 0.5% fibronectin and 0.02% gelatin 1h at 37°C (Sigma-Aldrich). To keep HL-1 phenotype, cell culture was maintained as previously described [20].

For hypoxia, cells were incubated at 37°C at 1%O_2.

HL-1 cardiomyocytes were transfected by siRNAs as follows: one day after being plated, cells were transfected with 10 nM of small interference RNAs from Dharmacon Acell SMARTpool targeting VASH1 (siVASH1) or non-targeting siRNA control (siControl), using Lipofectamine RNAiMax (Invitrogen) according to the manufacturer's recommendations, in a media without penicillin-streptomycin and norepinephrine. Cells were incubated 72h at 37°C with siRNA (siRNA sequences are provided in EV Table 5).

For lentivector transduction, 6.10^4 HL-1 cells were plated into each well of a 6-well plate and transduced overnight in 1 mL of transduction medium (OptiMEM-GlutaMAX, Life Technologies SAS) containing 5 µg/mL protamine sulfate in the presence of lentivectors (MOI 2). GFP-positive cells were quantified by flow cytometry analysis on a BD FACSVerse (BD Biosciences). HL-1 cells were transduced with an 80% efficiency.

Reporter activity assay

For reporter lentivectors, luciferase activities *in vitro* and *in vivo* were performed using Dual-Luciferase Reporter Assay (Promega, Charbonnières-les-Bains, France). Briefly, proteins from HL-1 cells were extracted with Passive Lysis Buffer (Promega France). Quantification of bioluminescence was performed with a luminometer (Centro LB960, Berthold, Thoiry, France).

RNA purification and RT-qPCR

Total RNA extraction from ischemic and healthy areas was performed using TRIzol reagent according to the manufacturer's instructions (Gibco BRL, Life Technologies, NY, USA). RNA quality and quantification were assessed by a Xpose spectrophotometer (Trinean, Gentbrugge, Belgium) and an automated electrophoresis system (Fragment Analyzer, Advanced Analytical Technologies, Paris, France).

500 ng RNA was used to synthesize cDNA using a High-Capacity cDNA Reverse Transcription Kit (Applied Biosystems, Villebon-sur-Yvette, France).

Gene expression was investigated using HOT Pol Evagreen qPCR Mix PLus (Euromedex, France) and performed on a StepOne sequence detection system (Applied Biosystems). 18S rRNA was used as a reference gene and all data were normalized based on 18S rRNA level. Relative quantification (RQ) of gene expression was calculated using the $2^{-\Delta\Delta CT}$ method. When the RQ value was inferior to 1, the fold change was expressed as -1/RQ. The oligonucleotide primers used are detailed in EV Table 4.

qPCR array

The DELTAgene Assay™ was designed by Fluidigm Corporation (San Francisco, USA). The qPCR-array was performed on BioMark with the Fluidigm 96.96 Dynamic Array following the manufacturer's protocol (Real-Time PCR Analysis User Guide PN 68000088). The list of primers is provided in EV Table 4. A total of 1.25ng of cDNA was preamplified using PreAmp Master Mix (Fluidigm, PN 100-5580, 100-5581, San Francisco, USA) in the plate thermal cycler at 95°C for 2min, 10 cycles at 95°C for 15sec and 60°C for 4min. The preamplified cDNA was treated by endonuclease I (New England BioLabs, PN M0293L, Massachusetts, USA) to remove unincorporated primers.

The preamplified cDNA was mixed with 2x SsoFast EvaGreen Supermix (BioRad, PN 172-5211, California, USA), 50µM of mixed forward and reverse primers and sample Loading Reagent (Fluidigm, San Francisco, USA). The sample was loaded into the Dynamic Array 96.96 chip (Fluidigm San Francisco, USA). The qPCR reactions were performed in the BioMark RT PCR system. Data was analyzed using the BioMark RT-PCR Analysis Software Version 2.0.

Polysomal RNA preparation

HL-1 cells were cultured in 150-mm dishes. 15 min prior to harversting, cells were treated by cycloheximide at 100 µg/ml. Cells were washed three times in PBS cold containing 100 µg/mL cycloheximide and scraped in the PBS/cycloheximide. After centrifugation at 3,000 rpm for 2 min at 4°C, cells were lysed by 450µl hypotonic lysis buffer (5 mM Tris-HCL, pH7.5 ; 2.5 mM $MgCl_2$; 1.5 mM KCl). Cells were centrifuged at 13,000 rpm for 5 min at 4°C, the supernatants were collected and loaded onto a 10-50% sucrose gradient. The gradients were centrifuged in a Beckman SW40Ti rotor at 39,000 rpm for 2.5 h at 4°C without brake. Fractions were collected using a Foxy JR ISCO collector and UV optical unit type 11. RNA was purified from pooled heavy fractions containing polysomes, as well as from light fractions containing free RNA.

Preparation of biotinylated RNA

The FGF1, VEGFA or EMCV IRESs was cloned in pSCB-A-amp/kan plasmid (Agilent) downstream from the T7 sequence. The plasmid were linearized and *in vitro* transcription was performed with MEGAscript T7 kit (Ambion), according to the manufacturer's protocol, in the presence of Biotin-16-UTP at 1 mM (Roche), as previously described [25]. The synthesized RNA was purified using RNeasy kit (Qiagen).

BIA-MS experiments

BIA-MS studies based on surface plasmonic resonance (SPR) technology were performed on BIAcore T200 optical biosensor instrument (GE Healthcare), as described previously **[12,25]**. Immobilization of biotinylated IRES RNAs was performed on a streptavidin-coated (SA) sensorchip in HBS-EP buffer (10 mM Hepes pH 7.4, 150 mM NaCl, 3 mM EDTA, 0.005% surfactant P20) (GE Healthcare). All immobilization steps were performed at a flow rate of 2 μl/min with a final concentration of 100 μg/ml.

Binding analyses were performed with normoxic or hypoxic cell protein extracts at 100 μg/ml over the immobilized IRES RNA surface for 120 sec at a flow rate of 30 μl/min. The channel (Fc1) was used as a reference surface for non-specific binding measurements. The recovery wizard was used to recover selected proteins from cell protein extracts. This step was carried out with 0.1% SDS. Five recovery procedures were performed to get enough amounts of proteins for MS identification.

Eluted protein samples from BIA experiment were digested *in gel* with 1 μg of trypsin (sequence grade, Promega) at 37°C OVN. Peptides were then subjected to LC-MS/MS analysis. The peptides mixtures were loaded on a YMC-Triart C18 150x300 μm capillary column (particle diameter 3 μm) connected to a RS3000 Dionex HPLC system. The run length gradient (acetonitrile and water) was 30 minutes. Then, on the AB Sciex 5600+ mass spectrometer, data were acquired with a data dependent analysis. Data were then loaded on Mascot software (Matrix Science) that attributes peptide interpretations to MS/MS recorded scans.

Surface Plasmon Resonance assays.

For kinetic analysis, immobilization of biotinylated FGF1 IRES RNA was performed on a streptavidin-coated (SA) sensorchip in HBS-EP buffer (10 mM Hepes pH 7.4, 150 mM NaCl, 3mM EDTA, 0.005% surfactant P20) (GE Healthcare). Immobilization step was performed at a flow rate of 2 µl/min with a final concentration of 100 µg/ml. Total amount of immobilized FGF1 IRES RNA was 1500 RU.

Binding analyses were performed with recombinant protein VASH1 (Abnova H00022846-P01) at 100 µg/ml over the immobilized FGF1. This recombinant VASH1 contains the 27 kDa N-terminal part of the protein coupled to glutathione S-transferase. The channel (Fc1) was used as a reference surface for non-specific binding measurements.

A Single-Cycle Kinetics (SCK) analysis to determine association, dissociation and affinity constants (ka, kd, and KD respectively) was carried out by injecting different protein concentrations (16.25 nM-300 nM). Binding parameters were obtained by fitting the overlaid sensorgrams with the 1:1. Langmuir binding model of the BIAevaluation software version 3.0.

Immunocytology

Cells were plated on glass coverslip and incubated for 4 h of normoxia or hypoxia. They were fixed with cold methanol at -20°C during 5 min, washed 3 times with PBS and permeabilized 1 min with 0.1% Triton. Then, cells were incubated 5 min with blocking solution (1% FBS, 0.5% BSA) and 3° min with anti-VASH1 antibody (1/50; sc-365541) and Alexa 488 conjugated anti-mouse secondary antibody. Images were acquired with LSM780 Zeiss confocal microscope, camera lens x60 with Z acquisition of 0.36 µM. A single plan is shown Fig. 6C.

Statistical analysis

All statistical analyses were performed using a two-tailed Student's t-test or one-way ANOVA and are expressed as mean +- standard error of the mean, *p<0.05, **p<0.01, ***<0.001, ****<0.0001.

ACKNOWLEDGMENTS
Our thanks go to J.J. Maoret and F. Martin from the Inserm UMR1048 GeT-TQ plateau of the GeT plateform Genotoul (Toulouse), F. Lopez and L. Tonini from the proteomic platform genotoul (Toulouse), J. Iacovoni from the Inserm UMR 1048 bioinformatics plateau, as well as L. van den Berghe and C. Segura from the Inserm UMR1037 vectorology plateau (Toulouse). We also thank W. Claycomb for providing HL-1 cells.

This work was supported by Région Midi-Pyrénées, Association Française contre les Myopathies (AFM-Téléthon), Association pour la Recherche sur le Cancer (ARC), European funding (REFBIO). F.H. had fellowships from the Région Midi-Pyrénées and from the Ligue Nationale Contre le Cancer (LNCC). E.R.G. had a fellowship from AFM-Telethon. A.C. Godet had a fellowship from LNCC.

EXPANDED VIEW MATERIAL
EV Figure 1, 2 and 3, EV Tables 1, 2, 3, 4, 5

REFERENCES
1. Pouyssegur J, Dayan F, Mazure NM (2006) Hypoxia signalling in cancer and approaches to enforce tumour regression. *Nature* 441: 437-443

2. Morfoisse F, Kuchnio A, Frainay C, Gomez-Brouchet A, Delisle MB, Marzi S, Helfer AC, Hantelys F, Pujol F, Guillermet-Guibert J, Bousquet C, Dewerchin M, Pyronnet S, Prats AC, Carmeliet P, Garmy-Susini B (2014) Hypoxia induces VEGF-C expression in metastatic tumor cells via a HIF-1alpha-independent translation-mediated mechanism. *Cell Rep* 6: 155-167

3. Holcik M, Sonenberg N (2005) Translational control in stress and apoptosis. *Nat Rev Mol Cell Biol* 6: 318-327

4. Forsythe JA, Jiang BH, Iyer NV, Agani F, Leung SW, Koos RD, Semenza GL (1996) Activation of vascular endothelial growth factor gene transcription by hypoxia-inducible factor 1. *Mol Cell Biol* 16: 4604-4613

5. Pages G, Pouyssegur J (2005) Transcriptional regulation of the Vascular Endothelial Growth Factor gene--a concert of activating factors. *Cardiovasc Res* 65: 564-573

6. Conte C, Riant E, Toutain C, Pujol F, Arnal JF, Lenfant F, Prats AC (2008) FGF2 translationally induced by hypoxia is involved in negative and positive feedback loops with HIF-1alpha. *PLoS One* 3: e3078

7. Baird SD, Turcotte M, Korneluk RG, Holcik M (2006) Searching for IRES. *RNA* 12: 1755-1785

8. Spriggs KA, Stoneley M, Bushell M, Willis AE (2008) Re-programming of translation following cell stress allows IRES-mediated translation to predominate. *Biol Cell* 100: 27-38

9. Faye MD, Holcik M (2015) The role of IRES trans-acting factors in carcinogenesis. *Biochim Biophys Acta* 1849: 887-897

10. Liberman N, Gandin V, Svitkin YV, David M, Virgili G, Jaramillo M, Holcik M, Nagar B, Kimchi A, Sonenberg N (2015) DAP5 associates with eIF2beta and eIF4AI to promote Internal Ribosome Entry Site driven translation. *Nucleic Acids Res* 43: 3764-3775

11. Mitchell SA, Spriggs KA, Coldwell MJ, Jackson RJ, Willis AE (2003) The Apaf-1 internal ribosome entry segment attains the correct structural conformation for function via interactions with PTB and unr. *Mol Cell* 11: 757-771

12. Morfoisse F, Tatin F, Hantelys F, Adoue A, Helfer AC, Cassant-Sourdy S, Pujol F, Gomez-Brouchet A, Ligat L, Lopez F, Pyronnet S, Courty J, Guillermet-Guibert J, Marzi S, Schneider RJ, Prats AC, Garmy-Susini BH (2016) Nucleolin Promotes Heat Shock-Associated Translation of VEGF-D to Promote Tumor Lymphangiogenesis. *Cancer Res* 76: 4394-4405

13. Lewis SM, Holcik M (2008) For IRES trans-acting factors, it is all about location. *Oncogene* 27: 1033-1035

14. Lewis SM, Veyrier A, Hosszu Ungureanu N, Bonnal S, Vagner S, Holcik M (2007) Subcellular relocalization of a trans-acting factor regulates XIAP IRES-dependent translation. *Mol Biol Cell* 18: 1302-1311

15. Huez I, Creancier L, Audigier S, Gensac MC, Prats AC, Prats H (1998) Two independent internal ribosome entry sites are involved in translation initiation of vascular endothelial growth factor mRNA. *Mol Cell Biol* 18: 6178-6190

16. Martineau Y, Le Bec C, Monbrun L, Allo V, Chiu IM, Danos O, Moine H, Prats H, Prats AC (2004) Internal ribosome entry site structural motifs conserved among mammalian fibroblast growth factor 1 alternatively spliced mRNAs. *Mol Cell Biol* 24: 7622-7635

17. Stein I, Itin A, Einat P, Skaliter R, Grossman Z, Keshet E (1998) Translation of vascular endothelial growth factor mRNA by internal ribosome entry: implications for translation under hypoxia. *Mol Cell Biol* 18: 3112-3119

18. Vagner S, Gensac MC, Maret A, Bayard F, Amalric F, Prats H, Prats AC (1995) Alternative translation of human fibroblast growth factor 2 mRNA occurs by internal entry of ribosomes. *Mol Cell Biol* 15: 35-44

19. Jain RK (2005) Normalization of tumor vasculature: an emerging concept in antiangiogenic therapy. *Science* 307: 58-62

20. Claycomb WC, Lanson NA, Jr., Stallworth BS, Egeland DB, Delcarpio JB, Bahinski A, Izzo NJ, Jr. (1998) HL-1 cells: a cardiac muscle cell line that contracts and retains phenotypic characteristics of the adult cardiomyocyte. *Proc Natl Acad Sci U S A* 95: 2979-2984

21. Kietzmann T, Roth U, Jungermann K (1999) Induction of the plasminogen activator inhibitor-1 gene expression by mild hypoxia via a hypoxia response element binding the hypoxia-inducible factor-1 in rat hepatocytes. *Blood* 94: 4177-4185

22. Ronkainen VP, Ronkainen JJ, Hanninen SL, Leskinen H, Ruas JL, Pereira T, Poellinger L, Vuolteenaho O, Tavi P (2007) Hypoxia inducible factor regulates the cardiac expression and secretion of apelin. *FASEB J* 21: 1821-1830

23. Morfoisse F, Renaud E, Hantelys F, Prats AC, Garmy-Susini B (2014) Role of hypoxia and vascular endothelial growth factors in lymphangiogenesis. *Mol Cell Oncol* 1: e29907

24. Creancier L, Morello D, Mercier P, Prats AC (2000) Fibroblast growth factor 2 internal ribosome entry site (IRES) activity ex vivo and in transgenic mice reveals a stringent tissue-specific regulation. *J Cell Biol* 150: 275-281

25. Ainaoui N, Hantelys F, Renaud-Gabardos E, Bunel M, Lopez F, Pujol F, Planes R, Bahraoui E, Pichereaux C, Burlet-Schiltz O, Parini A, Garmy-Susini B, Prats AC (2015) Promoter-Dependent Translation Controlled by p54nrb and hnRNPM during Myoblast Differentiation. *PLoS One* 10: e0136466

26. Sato Y (2012) The vasohibin family: Novel regulators of angiogenesis. *Vascul Pharmacol* 56: 262-266

27. Sato Y (2015) Novel Link between Inhibition of Angiogenesis and Tolerance to Vascular Stress. *J Atheroscler Thromb* 22: 327-334

28. Braunstein S, Karpisheva K, Pola C, Goldberg J, Hochman T, Yee H, Cangiarella J, Arju R, Formenti SC, Schneider RJ (2007) A hypoxia-controlled cap-dependent to cap-independent translation switch in breast cancer. *Mol Cell* 28: 501-512

29. Kishlyansky M, Vojnovic J, Roudier E, Gineste C, Decary S, Forn P, Bergeron R, Desplanches D, Birot O (2010) Striated muscle angio-adaptation requires changes in Vasohibin1 expression pattern. *Biochem Biophys Res Commun* 399: 359-364

30. Miyashita H, Watanabe T, Hayashi H, Suzuki Y, Nakamura T, Ito S, Ono M, Hoshikawa Y, Okada Y, Kondo T, Sato Y (2012) Angiogenesis inhibitor vasohibin1 enhances stress resistance of endothelial cells via induction of SOD2 and SIRT1. *PLoS One* 7: e46459

31. Durie D, Lewis SM, Liwak U, Kisilewicz M, Gorospe M, Holcik M (2011) RNA-binding protein HuR mediates cytoprotection through stimulation of XIAP translation. *Oncogene* 30: 1460-1469

32. Galban S, Kuwano Y, Pullmann R, Jr., Martindale JL, Kim HH, Lal A, Abdelmohsen K, Yang X, Dang Y, Liu JO, Lewis SM, Holcik M, Gorospe M (2008) RNA-binding proteins HuR and PTB promote the translation of hypoxia-inducible factor 1alpha. *Mol Cell Biol* 28: 93-107

33. Sato Y (2013) The vasohibin family: a novel family for angiogenesis regulation. *J Biochem* 153: 5-11

34. Sonoda H, Ohta H, Watanabe K, Yamashita H, Kimura H, Sato Y (2006) Multiple processing forms and their biological activities of a novel angiogenesis inhibitor vasohibin. *Biochem Biophys Res Commun* 342: 640-646

35. Kern J, Bauer M, Rychli K, Wojta J, Ritsch A, Gastl G, Gunsilius E, Untergasser G (2008) Alternative splicing of vasohibin1 generates an inhibitor of endothelial cell proliferation, migration, and capillary tube formation. *Arterioscler Thromb Vasc Biol* 28: 478-484

36. Shiroki K, Ohsawa C, Sugi N, Wakiyama M, Miura K, Watanabe M, Suzuki Y, Sugano S (2002) Internal ribosome entry site-mediated translation of Smad5 in vivo: requirement for a nuclear event. *Nucleic Acids Res* 30: 2851-2861

37. Stoneley M, Subkhankulova T, Le Quesne JP, Coldwell MJ, Jopling CL, Belsham GJ, Willis AE (2000) Analysis of the c-myc IRES; a potential role for cell-type specific trans-acting factors and the nuclear compartment. *Nucleic Acids Res* 28: 687-694

38. Xue S, Tian S, Fujii K, Kladwang W, Das R, Barna M (2015) RNA regulons in Hox 5' UTRs confer ribosome specificity to gene regulation. *Nature* 517: 33-38

39. Nanbru C, Lafon I, Audigier S, Gensac MC, Vagner S, Huez G, Prats AC (1997) Alternative translation of the proto-oncogene c-myc by an internal ribosome entry site. *J Biol Chem* 272: 32061-32066

40. Prats AC, Van den Berghe L, Rayssac A, Ainaoui N, Morfoisse F, Pujol F, Legonidec S, Bikfalvi A, Prats H, Pyronnet S, Garmy-Susini B (2013) CXCL4L1-fibstatin cooperation inhibits tumor angiogenesis, lymphangiogenesis and metastasis. *Microvasc Res* 89: 25-33

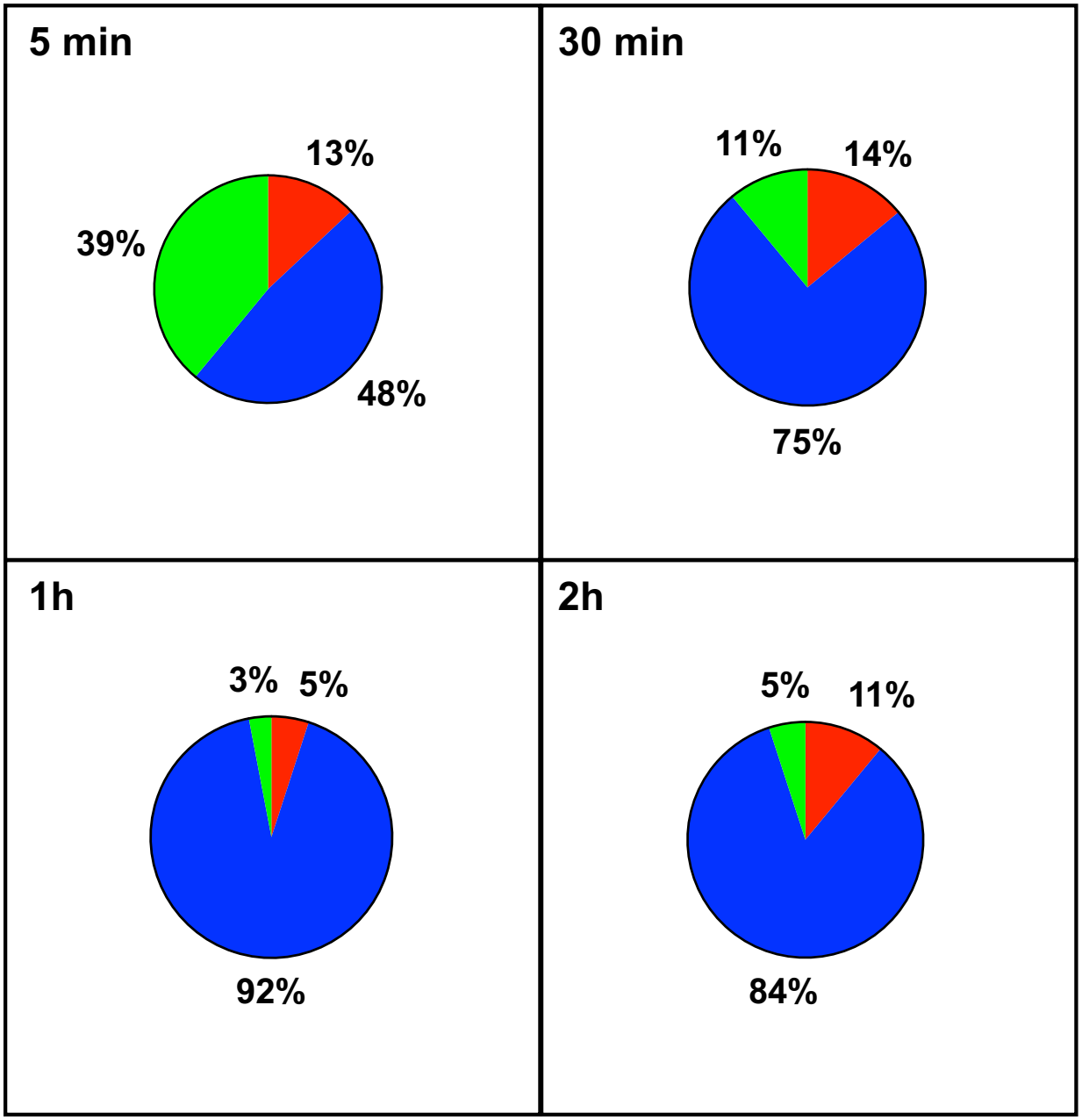

Expanded View Figure 1. Transcriptome of IRES-containing mRNAs in hypoxic cardiomyocytes.
Total RNA was purified from HL-1 cardiomyocytes submitted to increasing times from 5 min to 24 h of hypoxia at 1% O_2, as well as from normoxic cardiomyocytes as a control. cDNA was synthesized and used for a Fluidigm deltagene PCR array dedicated to genes related to (lymph)angiogenesis or stress (EV Table 4). Relative quantification (RQ) of gene expression during hypoxia was calculated using the $2^{-\Delta\Delta CT}$ method with normalization to 18S and to normoxia. The percentage of repressed (red), induced (green) and non-regulated (blue) mRNAs is shown for the earlier times of the kinetics. The later times are shown in Fig. 1. The detailed values for all the times of the kinetics are presented in EV Table 1.

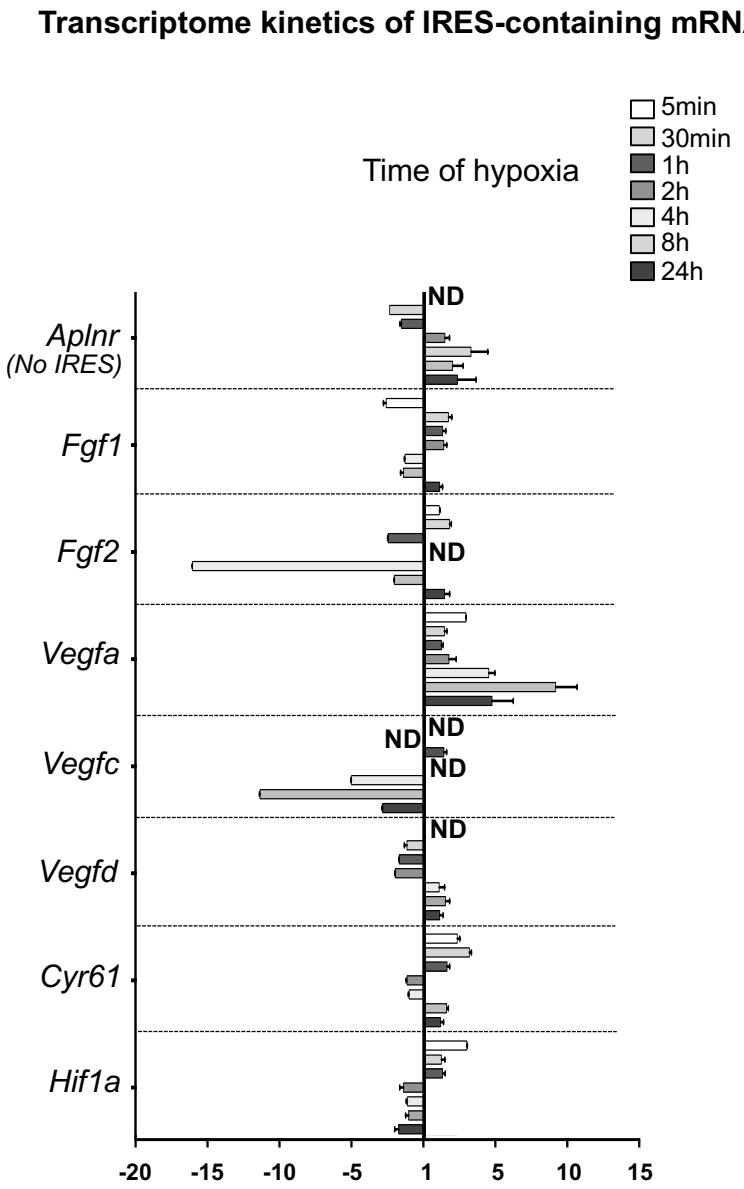

Expanded View Figure 2. Transcriptome of IRES-containing mRNAs in hypoxic cardiomyocytes.
RQ values for IRES-containing mRNA transcriptome kinetics extracted from the PCR arrays shown in EV Table 1. The gene *Aplnr* (apelin receptor) was chosen as a control without an IRES.

A

Mouse vasohibin-1 (NP_796328.2)

BindN prediction of RNA-binding residues

Summary

Input sequence length: 375 amino acids
Predicted binding sites: 125 residues
User-defined specificity: 80.00%
Estimated sensitivity: 53.95%

Overview

```
Sequence:     MPGGKKVVPSGSSSASPNAAATTTAAAAAAAAAPHSGTKRLETTEGASAQRDEEPEEEGE
Prediction:   ----++--++++++++++--+++---------+++++++-++++-++-++---------
Confidence:   433477326658884747523656444555433578789925666368266223446775

Sequence:     EDLRDGGVPFFINRGGLPVDEATWERMWKHVAKIHPDGEKVALRIRGATDLPKIPIPSVP
Prediction:   ---+---------+-----------+------+------+---+-+------+----+--
Confidence:   667677484669456552754634557525876723364552677645236367363464

Sequence:     TFQPTTPVPERLEAVQRYIRELQYNHTGTQFFEIKKSRPLTGLMDLAKEMTKEALPIKCL
Prediction:   +----+---------+---+---++-+--------+++--+--------------------
Confidence:   532325353428557424972724526324463726682357777872662265649389

Sequence:     EAVILGIYLTNSMPTLERFPISFKTYFSGNYFRHIVLGVNFGGRYGALGMSRREDLMYKP
Prediction:   -------------+--+-----+-+--+---+----------+---++-+++-------
Confidence:   699997939223644765757374345243486699979333382424626753234344

Sequence:     PAFRTLSELVLDYEAAYGRCWHVLKKVKLGQCVSHDPHSVEQIEWKHSVLDVERLGREDF
Prediction:   ---+-----------+-+--------+--+--+--------------------+--++--
Confidence:   343537459999866555603387228552656444533953856655886947447524

Sequence:     RKELERHARDMRLKIGKGTGPPSPTKDRKKDVSSPQRAQSSPHRRNSRSERRPSGEKKPA
Prediction:   ++---+--+--+-+--+-++++++++++++++++++++++++++++++++++++++++-
Confidence:   763527367357754382969999997898748757958999899999999988688863

Sequence:     EPKAMPDLSGYQIRV
Prediction:   +-+-----+-+--+-
Confidence:   524654575542878
```

*** Prediction: binding residues are labeled with '+' and in red; non-binding residues labeled with '-' and in green.
*** Confidence: from level 0 (lowest) to level 9 (highest).

B

Human vasohibin-1 (NP_055724.1)

BindN prediction of RNA-binding residues

Summary

Input sequence length: 365 amino acids
Predicted binding sites: 125 residues
User-defined specificity: 80.00%
Estimated sensitivity: 53.95%

Overview

```
Sequence:     MPGGKKVAGGGSSGATPTSAAATAPSGVRRLETSEGTSAQRDEEPEEEGEEDLRDGGVPF
Prediction:   ----++-++-+++++++++--++-+++-++--+++-++++++-----------+------
Confidence:   433377357259987857824564685498326672885774234467756676774846

Sequence:     FVNRGGLPVDEATWERMWKHVAKIHPDGEKVAQRIRGATDLPKIPIPSVPTFQPSTPVPE
Prediction:   --+-----------+------+------+---+-+-+------+---+---+-----+----
Confidence:   694565527546345575258767233644432657432363673634645323262434

Sequence:     RLEAVQRYIRELQYNHTGTQFFEIKKSRPLTGLMDLAKEMTKEALPIKCLEAVILGIYLT
Prediction:   -----+---+---++-+--------+++--+--------------------------------
Confidence:   285574249727245263244637266823577778726622656493896999979392

Sequence:     NSMPTLERFPISFKTYFSGNYFRHIVLGVNFAGRYGALGMSRREDLMYKPPAFRTLSELV
Prediction:   ---+-+---+--+-+---+---+-----+---++-+++-------+-----------+----
Confidence:   236447657573743452434866999793353735246267532343443435374599

Sequence:     LDFEAAYGRCWHVLKKVKLGQSVSHDPHSVEQIEWKHSVLDVERLGRDDFRKELERHARD
Prediction:   ------+-+---------+-+++-+--------------------+--++--++---+-+-
Confidence:   999766566833872285347445334339538566558869474474247635273673

Sequence:     MRLKIGKGTGPPSPTKDRKKDVSSPQRAQSSPHRRNSRSERRPSGDKKTSEPKAMPDLNG
Prediction:   -+-+--+-++++++++++++++++++++++++++++++++++++++++++++++-------
Confidence:   577543829699999978987487579589998999999999888989876576554725

Sequence:     YQIRV
Prediction:   ---+-
Confidence:   22778
```

C

cNLS Mapper Result (mouse VASH-1)

Predicted monopartite NLS		
Pos.	Sequence	Score
262	HVLKKVKLG	2.5

Predicted bipartite NLS		
Pos.	Sequence	Score
324	PTKDRKKDVSSPQRAQSSPHRRNSRSERRP	2.8
337	RAQSSPHRRNSRSERRPSGEKKPAEPKAMPDLSGY	2.2

D

cNLS Mapper Result (human VASH-1)

Predicted monopartite NLS		
Pos.	Sequence	Score
252	HVLKKVKLG	2.5

Predicted bipartite NLS		
Pos.	Sequence	Score
3	GGKKVAGGGSSGATPTSAAATAPSGVRRLE	2.8
4	GKKVAGGGSSGATPTSAAATAPSGVRRLET	2.8
76	RMWKHVAKIHPDGEKVAQRIRGATDLPKIPIPSVP	3
96	RGATDLPKIPIPSVPTFQPSTPVPERLEAVQRYI	2
141	FFEIKKSRPLTGLMDLAKEMTKEALPIKCLE	2
142	FEIKKSRPLTGLMDLAKEMTKEALPIKCLEA	3.7
222	RREDLMYKPPAFRTLSELVLDFEAAYGRCWHVLKK	2.2
231	PAFRTLSELVLDFEAAYGRCWHVLKKVKLG	2.1
249	RCWHVLKKVKLGQSVSHDPHSVEQIEWKHSVLDVE	2.7
296	RHARDMRLKIGKGTGPPSPTKDRKKDVSSPQRAQSS	3.5
314	PTKDRKKDVSSPQRAQSSPHRRNSRSERRP	2.8

Expanded View Figure 3. Conservation of predicted RNA binding domains and nuclear localization sequences (NLS) in mouse and human vasohibin-1.

A-B RNA binding domains in mouse (A) and human (B) VASH1 proteins were predicted using BindN software (https://omictools.com/bindn-2-tool)

C-D NLS were predicted using cNLS Mapper (http://nls-mapper.iab.keio.ac.jp/cgi-bin/NLS_Mapper_form.cgi/). Binding residues (red) are labeled with "+", non-binding residues (green) labeled with "-". The confidence level is indicated from level 0 (lowest) to 9 (highest).

The fully conserved monopartite NLS “HVLKKVKLG” identified in C and D has been positioned by a red box on the mouse and human peptide sequences shown in A and B, respectively.

Hantelys et al, EV Table 1

Hypoxia time	5min		30min		1h		2h		4h		8h		24h	
Gene name	**RQ**		**RQ**		**RQ**		**RQ**		**RQ**		**RQ**		**RQ**	
Akt1	1.60	±0.13	1.30	±0.06	1.20	±0.15	1.36	±0.25	-1.10	±0.09	1.40	±0.13	1.00	±0.32
Ang	2.65	±0.25	1.23	±0.36	-1.04	±0.12	1.24	±0.04	1.24	±0.12	1.09	±0.08	1.26	±0.28
Angpt1	5.51	±0.17	1.20	±0.30	1.19	±0.07	1.90	±0.49	2.43	±0.36	1.56	±0.43	-2.27	±0.06
Angptl4	1.03	±0.02	-3.14	±0.09	1.65	±0.54	1.60	±0.46	1.56	±0.67	3.50	±1.07	-1.37	±0.35
Anpep	ND		-3.26	±0.29	1.65	±0.01	-8.05	±0.06	-1.04	±0.14	1.62	±0.62	1.03	±0.43
Apln (Apelin)	2.11		-19,21	±0.01	-6.17	±0.05	-29.04	±0.01	36.77	±5.59	109.98	±6.98	335.72	±57.52
Aplnr	ND		-2.36	±0.03	-1.57	±0.10	1.44	±0.32	3.25	±1.70	1.98	±0.72	2.31	±1.29
Atp2a2 (SERCA2)	1.46	±0.08	1.21	±0.13	1.26	±0.14	1.50	±0.01	1.20	±0.06	1.84	±0.18	1.48	±0.32
Bai1	-1.52	±0.19	2.90	±0.91	1.17	±0.06	1.65	±0.52	1.36	±0.13	2.05	±0.60	1.04	±0.30
Ccl2	ND		-1.09	±0.49	1.76	±0.46	-2.76	±0.16	1.57	±1.01	2.99	±1.13	1.23	
Ccl21a	ND		-32.39	±0.01	2.97	±0.85	-1.90	±0.03	2.65	±2.78	-2.27	±0.21	1.32	±0.39
Col18a1	1.66	±0.71	1.58	±0.39	1.14	±0.14	1.45	±0.04	-1.69	±0.09	1.82	±0.43	1.57	±0.43
Col4a3	19.64	±0.07	1.52	±0.19	1.20	±0.21	1.31	±0.04	1.00	±0.03	1.45	±0.30	4.40	±0.80
Ctgf	1.29	±0.09	1.67	±0.26	1.16	±0.06	1.30	±0.13	1.06	±0.13	2.05	±0.30	3.66	±0.76
Cxcl1	1.32	±0.64	1.11	±0.27	1.67	±0.19	1.58	±0.12	1.01	±0.09	-1.43	±0.08	-2.04	±0.13
Cxcl10	1.37	±0.86	1.36	±0.29	1.11	±0.14	1.33	±0.25	1.05	±0.09	-1.02	±0.13	-1.08	±0.23
Cyr61	2.30	±0.18	3.14	±0.14	1.59	±0.18	-1.18	±0.07	-1.03	±0.06	1.56	±0.12	1.15	±0.21
Edn1	-2.43	±0.28	2.93	±0.31	1.72	±0.32	-1.4	±0.24	-1.39	±0.06	-1.33	±0.09	1.04	±0.26
Efna1	2.08	±0.15	1.23	±0.10	-1.52	±0.12	-1.16	±0.19	1.25	±0.09	1.17	±0.05	1.35	±0.33
Efnb2	1.74	±0.14	1.55	±0.25	1.14	±0.23	-1.03	±0.18	1.57	±0.18	3.71	±0.61	1.65	±0.42
Egf	ND		1.35	±0.14	1.32	±0.30	1.56	±0.44	1.56	±0.11	2.14	±0.53	-1.61	±0.35
Eng	2.96	±0.94	1.55	±0.39	1.18	±0.19	-1.02	±0.14	-1.11	±0.15	2.27	±0.33	1.65	±0.34
Ephb4	2.22	±0.13	1.67	±0.16	-1.03	±0.14	1.10	±0.13	1.01	±0.12	1.45	±0.09	1.57	±0.21
Erbb2 (Her2)	1.87	±0.19	1.85	±0.26	-1.01	±0.18	1.16	±0.18	1.32	±0.11	1.00	±0.18	1.34	±0.09
F3	1.12	±0.94	1.45	±0.18	1.28	±0.11	-1.57	±0.23	-1.23	±0.07	-1.09	±0.10	-1.56	±0.21
Fgf1 (aFGF)	-2.63	±0.18	1.69	±0.23	1.29	±0.22	1.37	±0.21	-1.32	±0.05	-1.43	±0.20	1.08	±0.20
Fgf2 (bFGF)	1.06	±0.04	1.76	±0.13	-2.5	±0.03	ND		-16.05	±0.02	-2.05	±0.07	1.43	±0.35
Fgfr3	1.41	±0.07	1.34	±0.27	-1.08	±0.12	1.38	±0.31	1.47	±0.27	3.93	±0.55	2.69	±0.39

Hypoxia time	**5min**		**30min**		**1h**		**2h**		**4h**		**8h**		**24h**	
Gene name	**RQ**		**RQ**		**RQ**		**RQ**		**RQ**		**RQ**		**RQ**	
Fn1	3.30	±0.07	1.70	±0.15	-1.02	±0.17	1.16	±0.01	-1.25	±0.06	2.45	±0.36	2.61	±0.49
Hif1a	2.97	±0.03	1.20	±0.24	1.28	±0.18	-1.42	±0.26	-1.15	±0.08	-1.06	±0.21	-1.75	±0.22
Hnrnpm	1.55	±0.18	1.17	±0.18	1.54	±0.15	2.26	±0.20	1.86	±0.25	3.86	±1.33	1.23	±0.26
Hpse	ND		3.23	±1.07	1.25	±0.34	1.64	±0.16	1.56	±0.14	3.52	±1.07	11.04	±1.95
Id1	-1.61	±1.12	1.58	±0.18	2.63	±0.50	3.01	±1.27	4.23	±0.19	2.01	±0.40	1.79	±0.64
Ifna1	ND		1.72	±0.17	-1.09	±0.06	1.73	±0.07	2.19	±0.33	3.11	±0.25	1.31	±0.49
Igf1	10.07	±0.59	1.54	±0.22	1.42	±0.15	1.06	±0.04	1.10	±0.22	-1.25	±0.14	-2.86	±0.14
Igf1r	ND		ND		ND		ND		-3.17	±0.08	2.37	±0.20	5.14	±0.32
Itgav	ND		1.19	±0.11	-1.36	±0.14	1.33	±0.29	1.33	±0.12	3.41	±0.56	2.82	±0.64
Itgb3	-4.33	±0.30	1.34	±0.19	-1.35	±0.02	1.04	±0.20	1.03	±0.20	1.42	±0.34	-1.37	±0.10
Jag1	2.13	±0.09	1.80	±0.24	1.03	±0.13	1.66	±0.46	1.46	±0.06	2.26	±0.37	1.76	±0.21
Mdk	1.14	±0.21	2.45	±0.17	-1.07	±0.17	-1.27	±0.00	1.16	±0.32	1.52	±0.38	-1.16	±0.46
Mmp14	-1.77	±0.03	1.30	±0.22	1.02	±0.06	-1.16	±0.17	1.06	±0.11	1.70	±0.24	1.95	±0.15
Mmp2	1.46	±0.18	1.96	±0.50	1.20	±0.05	1.68	±0.44	1.14	±0.33	1.94	±0.66	-1.23	±0.37
Neat1	4.03	±0.48	-1.17	±0.23	-1.59	±0.05	2.65	±0.00	1.89	±0.15	2.96	±1.02	-1.16	±0.29
Nos3	9.29		-4.01	±0.10	2.00	±0.54	-2.58	±0.26	-1.30	±0.14	-1.02	±0.40	-1.32	±0.19
Nrp1	2.46	±0.06	1.32	±0.17	1.04	±0.15	-1.25	±0.25	-1.10	±0.07	1.47	±0.25	1.10	±0.16
Nrp2	2.50	±0.07	1.55	±0.05	1.02	±0.12	1.02	±0.12	1.14	±0.19	1.72	±0.32	1.83	±0.39
P54nrb	2.96	±0.09	1.58	±0.42	1.21	±0.20	1.42	±0.29	1.22	±0.13	1.66	±0.30	1.11	±0.23
PAI1 (SerpinE1)	-1.73	±0.12	2.18	±0.54	1.46	±0.15	1.74	±0.65	5.75	±0.57	15.76	±2.01	13.18	±1.02
Pdgfa	3.65	±0.43	1.45	±0.18	1.29	±0.26	1.59	±0.36	1.71	±0.11	1.97	±0.35	1.54	±0.34
Pecam1	1.48		-11.55	±0.02	-1.09	±0.24	2.86	±1.08	2.09	±0.77	2.70	±1.72	2.60	±0.86
Pf4	ND		-39.36	±0.02	-1.79	±0.33	-2.20	±0.18	1.80	±0.40	1.48	±0.55	1.01	±0.28
Pgf	ND		2.17	±0.14	-1.36	±0.19	-7.89	±0.09	4.47	±0.89	1.85	±0.29	3.22	±0.85
Plau (upa)	1.13	±0.29	-1.04	±0.24	-1.36	±0.16	-1.31	±0.13	1.25	±0.30	1.58	±0.26	1.24	±0.24
Plg	ND		-2.71	±0.26	-1.05		2.45	±0.63	-1.35	±0.19	-3.33	±0.16	-2.94	±0.25
Prox1	7.13	±0.20	1.48	±0.23	1.26	±0.14	-1.13	±0.14	-1.08	±0.13	1.27	±0.29	-1.72	±0.07

Hypoxia time	**5min**		**30min**		**1h**		**2h**		**4h**		**8h**		**24h**	
Gene name	**RQ**		**RQ**		**RQ**		**RQ**		**RQ**		**RQ**		**RQ**	
Psf/Sfpq	1.45	±0.17	1.37	±0.09	1.30	±0.19	1.22	±0.08	1.10	±0.15	1.55	±0.59	-1.43	±0.16
Pspc1	1.00	±0.80	1.34	±0.11	1.50	±0.01	1.64	±0.58	1.67	±0.19	1.37	±0.31	1.59	±0.23
SerpinF1	ND		-31.89	±0.02	-9.09	±0.01	-1.91	±0.33	-2.38	±0.11	-1.14	±0.17	1.02	±0.37
Sphk1	ND		1.91	±0.80	1.70	±0.04	-1.51	±0.19	1.30	±0.11	2.78	±1.20	1.17	±0.43
Tek	1.97	±1.55	1.98	±0.23	1.55	±0.41	1.48	±0.20	1.24	±0.14	-1.25	±0.09	1.04	±0.13
Tgfa	ND		-2.01	±0.13	-7.94	±0.05	-6.9	±0.03	2.91	±0.63	3.50	±1.29	4.05	±1.71
Tgfb1	-5.26	±0.02	1.22	±0.23	-1.45	±0.14	1.03	±0.10	-1.02	±0.22	1.45	±0.24	1.05	±0.25
Tgfb2	-2.45	±0.08	1.50	±0.31	1.22	±0.07	1.37	±0.12	1.78	±0.24	2.00	±0.39	1.43	±0.40
Tgfbr1	-2.03	±0.57	1.33	±0.16	1.28	±0.25	1.48	±0.14	1.86	±0.34	2.23	±0.77	-1.27	±0.16
Thbs1	2.65	±0.09	1.88	±0.12	1.19	±0.09	1.47	±0.33	1.12	±0.07	1.30	±0.22	1.44	±0.08
Thbs2	2.15	±0.12	1.52	±0.10	1.03	±0.16	1.20	±0.18	-1.20	±0.01	1.21	±0.15	-1.22	±0.21
Timp1	-2.20	±0.04	1.13	±0.27	-1.32	±0.29	-1.96	±0.17	-1.28	±0.12	-1.22	±0.11	-2.33	±0.19
Timp2	2.21	±0.04	1.46	±0.22	1.14	±0.01	1.13	±0.09	1.67	±0.13	1.28	±0.12	-1.69	±0.15
Timp3	ND		2.70	±0.43	1.40	±0.23	1.98	±0.46	1.09	±0.16	1.04	±0.29	1.11	±0.17
Vash1	ND		ND		ND		ND		-3.01	±0.14	1.56	±0.30	1.10	±0.08
Vegfa	2.90	±0.02	1.40	±0.18	1.20	±0.12	1.72	±0.50	4.48	±0.43	9.12	±1.48	4.71	±0.69
Vegfb	1.38	±0.04	1.33	±0.10	-1.2	±0.11	1.02	±0.04	-1.09	±0.07	1.04	±0.22	-1.59	±0.10
Vegfc	ND		ND		1.38	±0.18	ND		-5.03	±0.05	-11.37	±0.03	-2.86	±0.16
Vegfd	ND		-1.19	±0.17	-1.73	±0.22	-1.99	±0.23	1.05	±0.37	1.48	±0.29	1.08	±0.24
Vegfr2 (Kdr)	-2.05	±0.05	1.25	±0.13	1.07	±0.04	1.43	±0.21	1.31	±0.10	2.29	±0.38	-1.01	±0.30

EV Table 1. Transcriptome of (lymph)angiogenic factor genes in hypoxic HL-1 cardiomyocytes.
Total RNA was purified from HL-1 cardiomyocytes submitted to increasing times from 5 min to 24 hr of hypoxia at 1% O_2, as well as from normoxic cardiomyocytes as a control. cDNA was synthesized and used for a Fluidigm deltagene PCR array dedicated to genes related to (lymph)angiogenesis or stress (EV Table 4). Relative quantification (RQ) of gene expression in hypoxia was calculated using the $2^{-\Delta\Delta CT}$ method with normalization to 18S and to normoxia. Standard deviation is indicated. When the RQ value is inferior to 1, the fold change is expressed as -1/RQ. ND means “non detected”.

Hantelys et al, EV Table 2

	Polysomes in hypoxia (4h)		SiVASH1 polysomes in normoxia	
Gene name	**RQ***	ST DEV	**RQ***	ST DEV
Akt1	2.07	0.07	-1.08	0.10
Ang	2.42	0.53	1.77	0.47
Angpt1	2.35	0.67	-1.27	0.10
Angptl4	3.26	1.56	-3.02	0.01
Anpep	3.41	0.21	1.10	0.20
Apln (Apelin)	1.71	0.27	-12.53	0.01
Aplnr	-2.89	0.11	ND	ND
Atp2a2 (SERCA2)	1.94	0.34	-1.30	0.15
Bai1	3.80	0.89	ND	ND
Ccl2	ND	ND	ND	ND
Ccl21a	ND	ND	ND	ND
Col18a1	2.64	0.61	-2.05	0.11
Col4a3	2.36	0.41	1.70	0.29
Ctgf	3.15	0.49	-2.66	0.05
Cxcl1	2.21	0.30	-1.61	0.25
Cxcl10	3.96	1.43	-16.36	0.02
Cyr61	2.00	0.24	-1.11	0.14
Edn1	2.49	0.55	2.54	0.19
Efna1	2.29	0.29	-1.42	0.14
Efnb2	2.48	0.71	-1.41	0.03
Egf	2.46	1.56	-2.68	0.12
Eng	2.71	0.78	-1.36	0.01
Ephb4	1.87	0.23	-1.33	0.00
Erbb2 (her2)	2.02	0.24	-1.39	0.11
F3	2.48	0.51	2.09	0.44
Fgf1 (aFGF)	2.56	0.87	-1.99	0.11
Fgf2 (bFGF)	ND	ND	ND	ND
Fgfr3	2.15	0.41	-1.89	0.05
Fibrillarin	ND	ND	-1.60	0.10
Fn1	2.34	0.30	-2.46	0.10
Hif1a	1.88	0.36	1.38	0.16
Hif2a	ND	ND	-2.21	0.03
Hnrnpm	2.48	0.50	1.01	0.17
Hpse	4.17	0.79	-13.33	0.02
Id1	1.93	0.38	ND	ND
Ifna1	3.93	1.38	ND	ND
Igf1	2.03	0.54	2.71	1.08
Igf1r	1.88	0.06	-1.47	0.04

	Polysomes in hypoxia (4h)		SiVASH1 polysomes in normoxia	
Gene name	**RQ***	ST DEV	**RQ***	ST DEV
Itgav	1.79	0.31	-1.17	0.13
Itgb3	2.44	0.40	1.96	0.20
Jag1	2.03	0.38	ND	ND
Mdk	2.03	0.35	ND	ND
Mmp14	1.85	0.18	1.38	0.02
Mmp2	1.91	0.44	ND	ND
Neat1	3.98	1.24	-2.86	0.05
Nos3	-1.29	0.10	-4.54	0.08
Nrp1	1.67	0.22	1.21	0.09
Nrp2	1.88	0.18	-1.28	0.14
P54nrb	3.12	0.78	-1.38	0.01
PAI1 (SerpinE1)	1.92	0.27	ND	ND
Pdgfa	2.42	0.48	-1.11	0.10
Pecam1	2.15	1.37	-2.53	0.01
Pf4	1.97	1.07	-3.75	0.03
Pgf	2.36	0.83	-1.71	0.04
Plau (upa)	2.16	0.50	-1.53	0.05
Plg	-3.83	0.21	ND	ND
Prox1	2.22	0.27	2.24	0.52
Psf/Sfpq	2.74	0.80	1.85	0.20
Pspc1	2.19	0.43	-2.27	0.08
SerpinF1	5.70	2.05	-2.32	0.15
Sphk1	-1.29	0.12	-3.82	0.04
Tek	2.43	0.95	12.03	3.59
Tgfa	2.45	0.31	ND	ND
Tgfb1	2.52	0.31	-2.27	0.03
Tgfb2	2.39	0.39	4.51	0.55
Tgfbr1	1.86	0.57	-1.10	0.17
Thbs1	2.03	0.30	7.48	2.32
Thbs2	1.98	0.28	-1.38	0.08
Timp1	2.36	0.34	1.24	0.34
Timp2	2.55	0.42	1.91	0.10
Timp3	1.95	0.31	-1.70	0.17
Vash1	6.86	1.27	ND	ND
Vegfa	2.95	0.70	1.41	0.19
Vegfb	2.85	0.43	1.40	0.21
Vegfc	ND	ND	ND	ND
Vegfd (Figf)	2.44	0.96	2.90	0.39
Vegfr2 (Kdr)	2.29	0.55	-1.35	0.15

EV Table 2. Translatome of (lymph)angiogenic factor genes in hypoxic HL-1 and in VASH1 knocked-down HL-1 cardiomyocytes. Polysomes were purified on sucrose gradient from HL-1 cardiomyocytes in normoxia or after 4 h of hypoxia at 1% O_2, or after treatment with siRNAs siControl and siVASH1 as described in Materials and Methods. RNA was purified from polysome-bound and free RNA. cDNA and PCR array was performed as in Figure 1 and in EV Table S1. Relative quantification (RQ) of gene expression in hypoxia was calculated using the $2^{-\Delta\Delta CT}$ method (polysomal RNA/free RNA normalized to normoxia). Standard deviation is indicated. When the RQ value is inferior to 1, the fold change is expressed as -1/RQ. ND means "non detected".

Hantelys et al, EV Table 3

A: BIA-MS data: HL-1 proteins bound to the FGF1 IRES RNA

	Normoxia		
ID	**Description**	**Score**	**Peptides**
ASAP2_MOUSE	Arf-GAP with SH3 domain, ANK repeat and PH domain-containing protein 2	48	1
EMAL6_MOUSE	Echinoderm microtubule-associated protein-like 6	43	1
FXL14_MOUSE	F-box/LRR-repeat protein 14	15	1
BRCC3_MOUSE	Lys-63-specific deubiquitinase BRCC36	20	1
MYBA_MOUSE	Myb-related protein A	26	1
NUDC2_MOUSE	NudC domain-containing protein 2	17	1
GUF1_MOUSE	Translation factor Guf1, mitochondrial	25	1
TMPSD_MOUSE	Transmembrane protease serine 13	15	1

	Hypoxia 4h		
ID	**Description**	**Score**	**Peptides**
ASAP2_MOUSE	Arf-GAP with SH3 domain, ANK repeat and PH domain-containing protein 2	51	2
ATPA_MOUSE	ATP synthase subunit alpha, mitochondrial	52	2
C2C2L_MOUSE	C2 domain-containing protein 2-like	25	2
PDE8B_MOUSE	High affinity cAMP-specific and IBMX-insensitive 3~,5~-cyclic phosphodiesterase 8B	23	1
GVIN1_MOUSE	Interferon-induced very large GTPase 1	29	1
ACOX1_MOUSE	Peroxisomal acyl-coenzyme A oxidase 1	23	1
TAM41_MOUSE	Phosphatidate cytidylyltransferase, mitochondrial	23	1
ALBU_MOUSE	Serum albumin	35	1
TCPG_MOUSE	T-complex protein 1 subunit gamma	28	1
VASH1_MOUSE	Vasohibin-1	26	1

	Hypoxia 8h		
ID	**Description**	**Score**	**Peptides**
ACTA_MOUSE	Actin, aortic smooth muscle	36	1
ADT1_MOUSE	ADP/ATP translocase 1	32	1
ASAP2_MOUSE	Arf-GAP with SH3 domain, ANK repeat and PH domain-containing protein 2	51	2
C2C2L_MOUSE	C2 domain-containing protein 2-like	32	1
CSPRS_MOUSE	Component of Sp100-rs	23	1
MCM8_MOUSE	DNA helicase MCM8	25	1
EMAL6_MOUSE	Echinoderm microtubule-associated protein-like 6	34	1
GKAP1_MOUSE G	kinase-anchoring protein 1	26	1
H1T_MOUSE	Histone H1t	41	1
ALBU_MOUSE	Serum albumin	41	1
SPE39_MOUSE	Spermatogenesis-defective protein 39 homolog	20	1
GUF1_MOUSE	Translation factor Guf1, mitochondrial	22	1
VASH1_MOUSE	Vasohibin-1	28	1

B: BIA-MS data: HL-1 proteins bound to the VEGF-Aa IRES RNA

	Normoxia		
ID	**Description**	**Score**	**Peptides**
ATPA_MOUSE	ATP synthase subunit alpha, mitochondrial	912	16
ATPO_MOUSE	ATP synthase subunit O, mitochondrial	374	7
ATPB_MOUSE	ATP synthase subunit beta, mitochondrial	372	8
ADT2_MOUSE	ADP/ATP translocase 2	364	5
HNRPU_MOUSE	Heterogeneous nuclear ribonucleoprotein	348	9
ACTA_MOUSE	Actin, aortic smooth muscle	147	1
ECHA_MOUSE	Trifunctional enzyme subunit alpha, mitochondrial	134	8
ACTB_MOUSE	Actin, cytoplasmic 1	119	1
ALBU_MOUSE	Serum albumin	100	1
NX SUCA_MOUSE	Succinyl-CoA ligase [ADP/GDP-forming] subunit alpha, mitochondrial	86	1
ATPG_MOUSE	ATP synthase subunit gamma, mitochondrial	78	1
THIM_MOUSE	3-ketoacyl-CoA thiolase, mitochondrial	57	1
SERPH_MOUSE	Serpin H1	54	1
ASAP2_MOUSE	Arf-GAP with SH3 domain, ANK repeat and PH domain-containing protein 2	52	1
PTRF_MOUSE	Polymerase I and transcript release factor	51	1
AT2A2_MOUSE	Sarcoplasmic/endoplasmic reticulum calcium ATPase 2	4	1
ILF2_MOUSE	Interleukin enhancer-binding factor 2	43	2
MOCS3_MOUSE	Adenylyltransferase and sulfurtransferase MOCS3	39	1
MYOG_MOUSE	Myogenin	33	1
TAGAP_MOUSE	T-cell activation Rho GTPase-activating protein	27	1
CH60_MOUSE	60 kDa heat shock protein, mitochondrial	26	1
C2C2L_MOUSE	C2 domain-containing protein 2-like	25	1
EFC14_MOUSE	EF-hand calcium-binding domain-containing protein 14	24	1
SPIR1_MOUSE	Protein spire homolog 1	24	1
ATAD3_MOUSE	ATPase family AAA domain-containing protein 3	20	1

	4h hypoxia		
ID	**Description**	**Score**	**Peptides**
ATPA_MOUSE	ATP synthase subunit alpha, mitochondrial	42	1
ASAP2_MOUSE	Arf-GAP with SH3 domain, ANK repeat and PH domain-containing protein 2	38	1
RN181_MOUSE	E3 ubiquitin-protein ligase RNF181	30	1
DOC10_MOUSE	Dedicator of cytokinesis protein 10	26	1
NID2_MOUSE	Nidogen-2	26	1
C2C2L_MOUSE	C2 domain-containing protein 2-like	25	1
PLCL1_MOUSE	Inactive phospholipase C-like protein 1	21	1

	8h hypoxia		
ID	**Description**	**Score**	**Peptides**
SPTC2_MOUSE	Serine palmitoyltransferase 2	20	1
CCD66_MOUSE	Coiled-coil domain-containing protein 66	28	1

ASAP2_MOUSE	Arf-GAP with SH3 domain, ANK repeat and PH domain-containing protein 2	35	1
ATPA_MOUSE	ATP synthase subunit alpha, mitochondrial	60	1
PHRF1_MOUSE	PHD and RING finger domain-containing protein 1	41	1
OXR1_MOUSE	Oxidation resistance protein 1	26	1
KCTD9_MOUSE	BTB/POZ domain-containing protein KCTD9	24	1
BIK_MOUSE	Bcl-2-interacting killer	21	1

C: BIA-MS data: HL-1 proteins bound to the EMCV IRES RNA

	Normoxia		
ID	**Description**	**Score**	**Peptides**
LOX15_MOUSE	Arachidonate 15-lipoxygenase	23	1
ASAP2_MOUSE	Arf-GAP with SH3 domain, ANK repeat and PH domain-containing protein 2	88	1
KCTD9_MOUSE	BTB/POZ domain-containing protein KCTD9	23	1
BRCC3_MOUSE	Lys-63-specific deubiquitinase BRCC36	27	1
PCLO_MOUSE	Protein piccolo	24	1
RPAP1_MOUSE	RNA polymerase II-associated protein 1	23	1
ALBU_MOUSE	Serum albumin	73	1
GUF1_MOUSE	Translation factor Guf1, mitochondrial	24	1

	4h hypoxia		
ID	**Description**	**Score**	**Peptides**
ASAP2_MOUSE	Arf-GAP with SH3 domain, ANK repeat and PH domain-containing protein 2	81	1
KCTD9_MOUSE	BTB/POZ domain-containing protein KCTD9	23	1
NUDC2_MOUSE	NudC domain-containing protein 2	20	1
PLPL1_MOUSE	Patatin-like phospholipase domain-containing protein 1	24	1
TAM41_MOUSE	Phosphatidate cytidylyltransferase, mitochondrial	21	1
VASH1_MOUSE	Vasohibin-1	22	1

	8h hypoxia		
ID	**Description**	**Score**	**Peptides**
ASAP2_MOUSE	Arf-GAP with SH3 domain, ANK repeat and PH domain-containing protein 2	36	1
EMAL6_MOUSE	Echinoderm microtubule-associated protein-like 6	30	1
BRCC3_MOUSE	Lys-63-specific deubiquitinase BRCC36	24	1
RPAP1_MOUSE	RNA polymerase II-associated protein 1	23	1
VASH1_MOUSE	Vasohibin-1	26	1

EV Table 3. BIA-MS analysis of IRES-bound proteins in hypoxic cardiomyocytes.
Total cell extracts from normoxic or hypoxic HL-1 cardiomyocytes were injected into the BIAcore T200 optical biosensor device where biotinylated IRES RNAs had been immobilized. The list of bound proteins identified by mass spectrometry (LC-MS/MS) after tryptic digestion is shown for FGF1 (A), VEGF-Aa (B) or EMCV (C) IRESs, respectively. The score and the number of peptides identified is indicated.

Hantelys et al, EV Table 4

Target	Forward primer 5' to 3'	Reverse primer 5' to 3'
Akt1	AGAACTCTAGGCATCCCTTCC	CGTTGGCATACTCCATGACA
Ang	TCCTGACTCAGCACCATGAC	ACATCTTTGCAGGGTGAGGTTA
Angpt1	ACAACACCGGGAAGATGGAA	TTCACCAGAGGGATTCCCAAAA
Angpt2	GAACCAGACAGCAGCACAAA	TCGAGTCTTGTCGTCTGGTTTA
Angptl4	CTTGGGACCAAGACCATGAC	TGGCTACAGGTACCAAACCA
Anpep	TGGGACTTTGTCCGAAGCA	TCCCTGGATGAGATTGGCAAA
Apln (Apelin)	GCAGGAGGAAATTTCGCAGAC	ACTTGGCGAGCCCTTCAA
Aplnr	TTGACTGGCCTTTTGGAACC	GCAAAAGACACTGGCGTACA
Atp2a2	CGGTCCAAGAGTCTCCTTCTA	GCACAATCCACTCCATCGAA
Bai1	GGTCCTGAGAAGCAAACCAA	GACCATTCGTTCCAGTTTCCA
Ccl11(Eotaxin)	CAACAACAGATGCACCCTGAA	CACAGATCTCTTTGCCCAACC
Ccl2 (mcp-1)	AGCAGCAGGTGTCCCAAA	TTCTTGGGGTCAGCACAGAC
Ccl21a	GTCAGGACTGCTGCCTTAAGTA	GCTTCCTATAGCCTCGGACAA
Cdh5	AACGAGGACAGCAACTTCAC	TGGCATGCTCCCGATTAAAC
Col18a1	CAGGACCAAAGGGTGACAAA	TTCCAGGTGGAAGAGGTCAA
Col4a3	GCTGGTACAAAGGGCAACAA	TAAGCCTGGCAATCCATCCA
Ctgf	AAGCTGACCTGGAGGAAAACA	TGCAGCCAGAAAGCTCAAAC
Cxcl1	CCTGAAGCTCCCTTGGTTCA	TTCTCCGTTACTTGGGGACAC
Cxcl10 (Inp10)	ATCCGGAATCTAAGACCATCAAGAA	GCTCTCTGCTGTCCATCCA
Cxcl5 (ena78/lix)	GGCATTTCTGTTGCTGTTCAC	TGCGGCTATGACTGAGGAA
Cxcl9	AGCCCCAATTGCAACAAAAC	TCTTCACATTTGCCGAGTCC
Cyr61	CCACACCAAGGGGTTGGAA	CACAGGGTCTGCCTTCTGAC
Edn1	CCTGGACATCATCTGGGTCAA	AACGCTTGGACCTGGAAGAA
Efna1	TGGGCAAGGAGTTCAAGGAA	GCACTGGGATTCCTGATGGTA
Efnb2	TGCCAGACAAGAGCCATGAA	GTCTTGTTGGACCGTGATTCC
Egf	GGAGAGACTGCTGAGTGTCA	AGCCAGCACACACTCATCTA
Eng	AGGCATCCAACACCATCGAA	TCTAGCTGGACTGTGACCTCA
Ephb4	CCTCACGGAATTCATGGAGAAC	ACCAGCTGGATGACTGTGAA
Erbb2 (Her2)	ATTCTCAGACGCCGGTTCA	TTGGCCCCAAAGGTCATCA
F3	ACCCAAACCCACCAACTATACC	GTGTCTGTGGTCGAGAAGCA
Fgf1 (aFGF)	TGGACACCGAAGGGCTTTTA	GCATGCTTCTTGGAGGTGTAA
Fgf2 (bFGF)	TCTTCCTGCGCATCCATCC	GCACACACTCCCTTGATAGACA
Fgfr3	AGGATTTAGACCGCATCCTCAC	CCTGGCGAGTACTGCTCAAA
Flt1	TTGCACGGGAGAGACTGAAA	GCCAAATGCAGAGGCTTGAA
Fn1	CGTCATTGCCCTGAAGAACA	AAGGGTAACCAGTTGGGGAA
Hgf	CATCAAATGCCAGCCTTGGAA	TCTTTACCGCGATAGCTCGAA
Hif1a	TCGACACAGCCTCGATATGAA	TTCCGGCTCATAACCCATCA
Hnrnpm	GATGCCAACCATCTGAGCAAA	CCAAATCCTATGCCTTCCATTCC
Hpse	GCCTCGAGGGAAGACAGTTAAA	TGCCATGTAAGAGAGTCGATCAC

Id1	ACCCTGAACGGCGAGATCA	GATCGTCGGCTGGAACACA
Ifna1	TCCACCAGCAGCTCAATGAC	TCTTCCTGGGTCAGGGGAAA
Ifng	GGCACAGTCATTGAAAGCCTA	GCCAGTTCCTCCAGATATCCA
Igf1	GAGCTGGTGGATGCTCTTCA	CTCCGAATGCTGGAGCCATA
Igf1r	ATGGAGCCTGAGAACATGGA	CCTTGTGTCCTGAGTGTCTT
Il1b	TGGCAACTGTTCCTGAACTCA	GGGTCCGTCAACTTCAAAGAAC
Il6	CCAGAAACCGCTATGAAGTTCC	GTTGTCACCAGCATCAGTCC
Il8	GGCTACTGTTGGCCCAATTAC	GCTTCATTGCCGGTGGAAA
Itgav	AAAGGCAGATGGCAAGGGAA	GGCTCCCTTCTGCTTGAGTTTA
Itgb3	CCCACCACAGGCAATCAAAA	GCGTCAGCACGTGTTTGTA
Jag1	TCCCAAGCATGGGTCTTGTA	GATGCACTTGTCGCAGTACA
Lect1	CCTGCCGATTTTCTGGCTTA	AGAGGGAGCACTGTTTCTCA
Lep	AGACCATTGTCACCAGGATCA	ATGAAGTCCAAGCCAGTGAC
Mdk	TTGCCCTCTTGGTGGTCAC	CCAGGTCCACTCCGAACAC
Mmp14	CAAGGCTGATTTGGCAACCA	GCCTTGATCTCAGTCCCAAAC
Mmp2	CGAGGACTATGACCGGGATA	GGGCACCTTCTGAATTTCCA
Mmp9	TCCCCAAAGACCTGAAAACC	GGGTGTAACCATAGCGGTAC
Neat1	GGGAAGCTGATTGCCAAGAA	ATGGTTTCAGAGCCCACAAC
P54nrb	TGGTACTCCAGCTCCTCCA	CAGCTTGGCCAAAACGTTCA
Nos3	GGGATTCTGGCAAGACAGACTA	GCAGCCAAACACCAAAGTCA
Notch4	ACCTGCTTGCAACCTTCCA	GGTGCACTCATTGACCTCCA
Nrp1	CCTGTATCCTGGGAAACTGGTA	GCCCAACATTCCAGAGCAA
Nrp2	GTGGATCAGCAGCGCTAAC	GCCATCACTCTGCAGTTTCAA
PAI1 (serpinE1)	CAGACAATGGAAGGGCAACA	GAGGTCCACTTCAGTCTCCA
Pdgfa	TGTAACACCAGCAGCGTCAA	GGCTTCTTCCTGACATACTCCA
Pecam1	GCACAGTGATGCTGAACAAC	GTCACCTTGGGCTTGGATAC
Pf4	CCAGCCTGGAGGTGATCAA	GGCAAATTTTCCTCCCATTCTTCA
Pgf	CCAATCGGGATCCACATTTCTA	GCCTTTGTCGTCTCCAGAATA
Plau (upa)	TAGCCTAGGCCTGGGGAAA	AGGCCAATCTGCACATAGCA
Plg	TGGAATTGCCCACAGTTTCC	CCGATAGTCTTTGCCATTCCC
Prok2	GGCTTGGCGTGTTTAAGGAC	GGGTCGCATTTCAAGTTCCTAC
Prox1	GCCCTCAACATGCACTACAAC	CGTGATCTGCGCAACTTCC
Psf/Sfpq	TGAAAAGCTGGCCCAGAAGAA	TGTGCCATGCTGAGCAAAAC
Pspc1	TCCCCGTGGAGCAATAAACA	ATACCCATCATTGGAGGAGGAC
Ptgs1	TATCACCTGCGGCTCTTCAA	GTTCCACGGAAGGTGGGTA
S1pr1	CGGTGTAGACCCAGAGTCC	GAGAGGCCTCCGAGAAACA
SerpinF1	AGAACCTCAAGAGTGCTTCCA	TTCTCCAGAGGGGCAACAAA
Sphk1	GGCAGCTTCTGTGAACCACTA	CAGCAGGTTCATGGGTGACA
Tek	GTTGGATGGCAATCGAATCAC	CCAGAGCAATACACCATAGGAC
Tgfa	CCCTGGCTGTCCTCATTATCA	CAGTGTTTGCGGAGCTGAC
Tgfb1	GCTGCGCTTGCAGAGATTAA	GTAACGCCAGGAATTGTTGCTA
Tgfb2	GCCCATATCTATGGAGTTCAGACA	AGCGGAAGCTTCGGGATTTA

Tgfbr1	AATTGCTCGACGCTGTTCTA	ACCGATGGATCAGAAGGTACA
Thbs1	CCCCAGAAGACATTCTCAGGAA	CGTTCACCACGTTGTTGTCA
Thbs2	GACTGCACGTCATGGTGAAC	CCCAATGAGCTCCAAAAGGAAC
Tie1	CCTTTGCTCAGATCGCACTA	CTCAAACAGCGACATGTTCAC
Timp1	TCCCCAGAAATCAACGAGACC	CATTTCCCACAGCCTTGAATCC
Timp2	GAAGAGCCTGAACCACAGGTA	TCATCCGGGGAGGAGATGTA
Timp3	CCCTTTGGCACTCTGGTCTA	ACGTGGGGCATCTTACTGAA
Tnf	CAAATGGCCTCCCTCTCATCA	TGGGCTACAGGCTTGTCAC
Tymp	GGCACACTGGATAAGCTGGAA	CAGCAGCCGACTTCCTCAA
Vash1	GGCTGCCAAGTTGGGGTGTGTT	AAACCAGGGCGTGGCTCCTGTA
Vegfa	CCAGCACATAGGAGAGATGAG	CTGGCTTTGTTCTGTCTTTCTT
Vegfb	GAGATGTCCCTGGAAGAACACA	TGGCTTCACAGCACTCTCC
Vegfc	AGACGTTCTCTGCCAGCAA	AGGCATCGGCACATGTAGTTA
Vegfd (figf)	TCCATTCAGACCCCAGAAGAA	GTGTTATCCCACAGCATGTCA
Vegfr2 (Kdr)	ATTTCACCTGGCACTCTCCA	TCCCAGGAAAGGGTTTCACA
Vegfr3 (Flt4)	CTCGCTCGGGACATCTACAAA	GGGCCATCCATTTCAGAGGAA
18S	CAACTAAGAACGGCCATGCA	AGCCTGCGGCTTAATTTGAC

EV Table 4. List of genes and primer couples used in the Fluidigm Deltagene PCR array.

Hantelys et al, EV Table 5

siControl (5’ -> 3’)	siVASH1 (5’->3’)
ACCAAAUGUACAGCUGAUU	GACACUAGGACCCUUAAAU
ACCAAAUGUACAAAAGACU	CGAAGUUCUGGAUAAAGAG
ACCAAAUGUACAAAAGGAU	CCCUCCUGGACUACAUGUU
ACCAAAUGUACAACACACU	CAUGUUAGUGUGUCCCUGU

EV Table 5. SiRNA sequences. The sequences of the four siRNAs present in the siControl and siVASH1 Smartpools are indicated.